BMC Plant Biology

RESEARCH Open Access

CDPK protein in cotton: genomic-wide identification, expression analysis, and conferring resistance to heat stress

Wen-Ben Lv[1], Cheng-Cheng Miao[1], Cheng-Hao Du[1], Ya-Ting Cui[1], Man Liu[1], Mei-Chen Shen[1], Anane Gideon Owusu[1], Ning Guo[1], Da-Hui Li[1] and Jun-Shan Gao[1*]

Abstract

Background Calcium-dependent protein kinase (CDPK) plays a key role in cotton tolerance to abiotic stress. However, its role in cotton heat stress tolerance is not well understood. Here, we characterize the *GhCDPK* gene family and their expression profiles with the aim of identifying CDPK genes associated with heat stress tolerance.

Results This study revealed 48 *GhCDPK* members in the cotton genome, distributed on 18 chromosomes. Tree phylogenetic analysis showed three main clustering groups of the *GhCDPKs*. Cis-elements revealed many abiotic stress and phytohormone pathways conserved promoter regions. Similarly, analysis of the transcription factor binding sites (TFBDS) in the *GhCDPK* genes showed many stress and hormone related sites. The expression analysis based on qRT-PCR showed that *GhCDPK16* was highly responsive to high-temperature stress. Subsequent protein-protein interactions of *GhCDPK16* revealed predictable interaction with ROS generating, calcium binding, and ABA signaling proteins. Overexpression of *GhCDPK16* in cotton and *Arabidopsis* improved thermotolerance by lowering ROS compound buildup. Under heat stress, *GhCDPK16* transgenic lines upregulated heat-inducible genes *GhHSP70*, *GHSP17.3*, and *GhGR1*, as demonstrated by qRT-PCR analysis. Contrarily, *GhCDPK16* knockout lines in cotton exhibited an increase in ROS accumulation. Furthermore, antioxidant enzyme activity was dramatically boosted in the *GhCDPK16*-ox transgenic lines.

Conclusions The collective findings demonstrated that *GhCDPK16* could be a viable gene to enhance thermotolerance in cotton and, therefore, a potential candidate gene for improving heat tolerance in cotton.

Keywords Cotton, *CDPK* gene family, Heat stress, Tolerance

*Correspondence:
Jun-Shan Gao
gaojsh@ahau.edu.cn
[1]School of Life Sciences, Anhui Agricultural University, Hefei 230036, P. R. China

Background

Increasing high temperatures is an all-encompassing issue worldwide. In contrast to humans, plants are sessile, which limits their capacity to withstand the negative impacts of unfavorable environmental circumstances that lead to improper growth and development. High temperature is an unfavorable factor that not only impairs photosynthetic activity and negatively affects cell division and growth but also reduces the yield of crops, threatens food security, and endangers human life [1]. Plants undergo a series of morpho-anatomical and physiochemical processes when exposed to extreme high temperatures, resulting in high levels of reactive oxygen species (ROS) in cells and the accumulation of oxides such as H_2O_2 and malondialdehyde (MDA), exposing plants to oxidative damage during oxidative stress [2].

To re-stand the continual consequences of stress, plants engage in natural defensive cellular and molecular processes. The molecular mechanism of heat stress responses in plants is well understood. An existing library of genes linked to heat stress have been found and classified, including RNA helicases, heat shock proteins (Hsps), and ring finger proteins, which are involved in heat stress tolerance [3–5]. Non-coding RNAs, including as microRNAs (miRNAs) and long non-coding RNAs (lncRNAs), are also thought to influence heat stress responses [2, 6]. Furthermore, regulatory proteins, including CDPKs [7], wall associated receptor-like protein kinases (RLKs) [8], and mitogen-activated protein kinases are crucial for controlling signal transduction in heat-stressed conditions.

Enhancing plant adaptability to environmental stress, the mechanisms regulated by stimulation and subsequent signal transduction often trigger diverse chemical, molecular, biochemical, and physiological changes. Moreover, during stress encounters, plant cells employ the well-known calcium-dependent protein kinase (CDPK) sensor protein family to launch quick signal transduction pathways by inducing phosphorylation cascades [9]. A number of significant families of calcium ion binding proteins, such as calmodulin (CaM), CAM-like proteins (CML), calcineurin B-like proteins (CBL), and Ca^{2+}-dependent protein kinases (CDPK), have also been identified in plants [9, 10]. However, the CDPK family is the largest calcium-sensing family exclusive to plants, protozoa, oomycetes, and green algae [11]. In addition, they are encoded by a wide-ranging gene family that is important for the growth and development of plants, as well as their ability to resist biotic and abiotic stressors [9, 12]. For instance, CDPKs are highly responsive to cold stress in rice seedling stem tissues, involved in light signaling, positively regulate drought, and salt tolerance [13, 14]. Concerning high temperature tolerance, reports have shown that *Arabidopsis AtCPK3*, which is Ca^{2+}/CaM-dependent, activates HSF to trigger the expression of downstream HSPs that enhance heat tolerance in response to high-temperature stress [15]. *ZmCDPK7* is a heat-stress protein kinase involved in ABA signaling and heat-stress tolerance in maize [7], *VaCPK29* is involved in grapevine responses to heat stress [16], while *GhCDPK60* positively regulates drought stress tolerance in both transgenic *Arabidopsis* and cotton by controlling proline and ROS levels [17].

As a cash crop of global importance, cotton (*Gossypium hirsutum* L.) is crucial for national economic development [18]. Cotton thrives in warm temperatures and grows best at high temperatures ranging from 28 to 35 °C. However, temperatures over 35 °C harm cotton growth causing anther dehiscence, reduced pollen activity, and hampered reproductive process [4]. China, India, Pakistan, and Uzbekistan are the top cotton-producing nations, accounting for 80% of the world's cotton output [19, 20]. Nevertheless, regions with heavy cotton farming often experience temperatures exceeding 40 °C, leading to significant production losses per unit [19]. As a result, screening and breeding plant species for heat tolerance is crucial.

Previous research has identified CDPK in the cotton genome and its impact on fiber development and abiotic stress tolerance [17, 21]. Although the role of the CDPK family in regulating abiotic stress tolerance is well understood, its functional significance and characterization under heat stress are still unclear. To address this gap, we used various bioinformatics techniques, such as phylogenetic analysis, protein-protein interaction analysis, chromosomal distribution, exon-intron structures, collinearity analysis, and identification of cis-regulatory elements and binding sites for transcription factors (TF), to characterize the cotton CDPK protein in the cotton genome. Out of the 48 *GhCDPK* genes that were identified, *GhCDPK16* was found to be associated with heat stress tolerance and was selected for further investigation. Overexpression of *GhCDPK16* in *Arabidopsis* facilitated additional functional roles. The study revealed new information about cotton's ability to withstand heat stress and indicated that *GhCDPK16* could be a promising candidate for genetic improvement.

Methods

Databases and identification of CDPK gene families

The upland cotton genome-wide database was obtained from the website (http://mascotton.njau.edu.cn) [22]. The *Arabidopsis* genomic database source was obtained at the website (http://www.arabidopsis.org/). Using DNATOOLS software, a local database of the complete genome sequences of *Arabidopsis thaliana*, *Gossypium hirsutum*, *Oryza sativa*, and *Zea mays* was established. CDPK family genes were screened in the local database

using TblastN (E-value=0.001) for comparison against the structural domain of CDPK's kinase (PF00069. 16) in *A. thaliana*. Using the Pfam (http://pfam.xfam.org/) and NCBI (https://www.ncbi.nlm.nih.gov/Structure/cdd/wrpsb.cgi) databases, all downloaded sequences were subjected to domain search to screen the CDPK sequence gene signature domains (Pkinase, EF-hand). The confirmed CDPK sequences were subjected to multiple sequence alignment using the ClustalW tool in MEGA 6.0 [23].

Physicochemical properties and molecular structure

The ExPAsy (http://www.expasy.org/) online tool was utilized to examine the amino acid sequence, isoelectric point (PI), molecular weight (MW) of the protein, and number of exons. Prediction of N-terminal myristoylation was carried out using the Myristoylator tool (https://web.expasy.org/myristoylator/) [24]. Subcellular localization prediction of proteins was performed using Cell-PLoc 2.0 software (http://www.Csbio.sjtu.Edu.cn/bioinf/Cell-PLoc-2/).

Cis-acting elements of CDPK promoter

For the prediction of cis-acting elements in the promoter region of CDPK genes in *G. hirsutum*, a sequence located 2000 bp upstream of the coding sequence start site was analyzed using the PlantCARE (http://bioinformatics.psb.ugent.be/webtools/plantcare/html) online website.

Phylogenetic, gene structure, motif pattern and gene duplication of CDPKs

To conduct tree phylogeny, 152 CDPK protein sequences were used from four plant species including *G. hirsutum* (48), *A. thaliana* (34), *O. sativa* (30), and *Z. mays* (40). The MEGA6.0 software was used to perform multiple sequence alignment by utilizing the ClustalW 1.8.1 tool. The phylogenetic tree was constructed using the neighboring grouping method, and the p-distance, Jones-Taylor-Tornton (JTT) model, and Poisson model were employed for this purpose. Nonparametric bootstrapping values of 1000 replicates were used to ensure the reliability of the constructed tree [9]. The structure of exons and introns in the CDPK family of *G. hirsutum* was obtained by using the GSDS online tool (http://gss.cbi.pku.edu.cn/). Based on the protein sequence obtained, the MEME online analysis tool (http://meme.sdsc.edu/) was used to analyze the motif pattern of the CDPK family protein in *G. hirsutum* [25]. The Plant Genome Duplication Database (PGDD: http://chibba.agtec.uga.edu/duplication/) was used to extract synonymous (Ks) and nonsynonymous (Ka) substitution rates, followed by KaKs computation using the KaKs_Calculator2.0 of Tbtools as previously described [24].

Collinearity, synteny and chromosome localization

The duplication and intraspecific covariance of *GhCDPK* family members were analyzed using the one-step MCSanX-Super Fast function in TBtools [26]. The evolutionary relationship between pairs of CDPK genes was analyzed using TBtools advanced circos function. Furthermore, to map the chromosomal localization information of *G. hirsutum* and three other species (*A. thaliana*, *O. sativa* and *Z. mays*), the collinearity connection was established using MapInspect software (https://mapinspect.software.informer.com).

Transcription factor binding site analysis of the GhCDPK family

Putative TFBDS of the *GhCDPK* family were determined using the *G. hirsutum* genome database. The predicted TF binding sites in the target genes were analyzed using the Plant Transcriptional Regulatory Map website (http://plantregmap.gao-lab.org/) [27].

Functional network interaction

The online STRING 10 (https://string-db.org/) tool was used to predict the interaction network between *GhCDPK16* and interactive protein gene in *A. thaliana* and *G. hirsutum* based on text mining, databases, co-expression, neighborhood, gene fusion, co-occurrence, and experimental evidence [28].

Plant materials and heat treatment

The heat-sensitive upland cotton cultivar "FuZi mian" (18YZ589) was employed in this investigation. Seedlings were cultivated in a greenhouse, under optimal growth conditions of 24 °C with 16 h of light and 8 h of darkness. At the two true-leaf stages, seedlings of similar growth were selected and subjected to high-temperature stress treatment at 42 °C. Different samples were collected at different time intervals during a heat stress treatment. The collection times included 0 h of no stress, as well as 1, 2, 4, 8, and 12 h of heat stress. *A. thaliana* (Columbia) was grown in a conditioned greenhouse with a 16-hour/8-hour photoperiod at 22 °C and a relative humidity of 60%. Seeds of both wild-type and transgenic *GhCDPK16-ox Arabidopsis* lines were grown on MS plates to observe their response to heat stress treatments. The seeds were treated at 45 °C for 1 h and were then allowed to recover for 5 days for further observation. Next, 7-day-old seedlings of *GhCDPK16-ox Arabidopsis* lines and wild-type grown on MS plates were treated at 45 °C for 2 h and were then allowed to recover for 7 days for observation and survival rate was further analyzed. Afterwards, 4-week-old *GhCDPK16-ox Arabidopsis* lines and wild-type were grown in a soil medium and then subjected to 45 °C heat treatment for 24 h and the

phonological changes were observed to study the function of genes in response to stress.

SgRNA design, pRGEB32-*GhCDPKR16*-Cas9 construction and Agrobacterium-mediated transient expression in cotton

The nucleic acid sequence of *GhCDPK16* and the corresponding NGG structure were discovered in the CDS. The sgRNA primers for *GhCDPK16* were designed using (http://cbi.hzau.edu.cn/crispr) with the forward primer as 5'-TTCTATGGAGAAACTGAGCA-3' and the reverse primer as 5'-CTAAAGGTCATTTTTCAG GAG-3'. By one-step cloning method, the CRISPR-Cas9 knockout vector pRGEB32 [29] was enzymatically sliced with the restricted intracytoplasmic enzyme *Bsa*I, and the long fragment containing tRNA + target + gDNA was linked to the linear vector. The cloned vector was introduced into the DH5a competent cell; positive clones were selected, sequenced, and gene-editing expression vector pRGEB32-*GhCDPK16*-Cas9 was obtained.

The vectors (pCAMBIA1305-*GhXTH16* and pRGEB32-*GhCDPK16*-Cas9) were transformed into Agrobacterium GV3101, cultured at 28 °C in 200 µl Luria Bertani (LB) liquid medium with an appropriate amount of rifampicin and kanamycin until the OD_{600} = 1.5 and the bacterium was collected at 10,000 r/min. The mixtures were then resuspended with a transformation mixture containing 100 µmol/L acetylcholine (AS) and 10 mmol / L$MgSO_4$ to obtain the conversion liquid at an OD_{600} value of 0.6. Cultivated cotton seedlings were selected and sterilized with 75% ethanol and washed with distilled water to clear the residual alcohol. Subsequently, syringes without the needle were used to inject the vacuum side of the leaf blades, and then the injection sides were properly cleaned with a cotton swab dipped in distilled water. Finally, the injected cotton plants were cultured at 25 °C with a light and dark period of 16 h/ 8 h for 2–3 days. Each treatment consisted of at least 5 seedlings. Successfully transformed plants were validated through qRT-PCR and RT-PCR analysis.

Vector construction and arabidopsis genetic transformation

Vector and genetic transformation was carried out as previously described by [30] with few modifications. Briefly, the coding sequence of *GhCDPK16* was amplified using KOD One TM PCR Master Mix (Toyobo, Tokyo, Japan) with gene-specific forward and reverse primers ligated into the pCAMBIA1305 vector (Table S3). Next, the expression vector pCambia1305-*GhCDPK16* was introduced into Agrobacterium tumefaciens strain EHA105. The ecotype Col-0 *Arabidopsis* was used in genetic transformation by the floral dip method. Then the harvested T0 generation seeds were selected on 1/2 Murashige and Skoog (MS) medium with 50 mg/L kanamycin, and the resistant plants were further validated using PCR. Single-copy lines with a segregation ratio of 3:1 were selected and planted until the T3 generation. The transgenic *GhCDPK16-ox Arabidopsis* lines were grown in a growth chamber with a 16-h light/8-h dark scheme, and the growth temperature was set at around 22 °C.

RNA extraction and real-time quantitative PCR

Total RNA was isolated from fresh 0.1 g samples using the RNAprep Pure Plant Plus Kit (polysaccharides and polyphenolics-rich) according to the manufacturer's instructions. First-strand cDNAs were synthesized from 1 µg of total RNA using the StarScript III All-in-one RT Mix with gDNA Remover. Then, qRT-PCR analysis was performed from three biological replicates as previously described by [20]. The *GhUBQ* gene was used as a reference and the relative expression levels were calculated using the $2^{-\Delta\Delta Ct}$ method. The primer sequences used for the experiments are shown in Table S2.

H_2O_2 and MDA determination and histochemical staining

H_2O_2 content was measured based on the kit instruction method described previously by [31]. For MDA content determination, 0.5 g of plant leaves was weighed and ground together with 2 mL of phosphoric acid medium solution (PBS) on ice. Afterwards, the mixture was centrifuged at 8000 g for 10 min at a temperature of 4 °C. Next, the supernatant was extracted, and 3 mL of 5% thiobarbital acid was added, then placed in a water bath to boil for 10 min, cooled under 4 °C for 2 to 5 min, then centrifuged again to extract the supernatant. With water as the control, the absorbance was measured at 532 nm and 600 nm. For histochemical staining, leaves were chosen at random and submerged in diaminobenzidine (DAB) and nitro-blue tetrazolium (NBT) solutions, respectively. Chlorophyll was removed by using 95% ethanol, followed by soaking in 70% glycerin for microscopic observation and photography. This entire process was repeated three times and the intensity was quantified using ImageJ software [32].

Determination antioxidant enzyme parameters

To measure the levels of antioxidant enzyme activity, a 0.1 g sample of leaf was ground with 1 mL of ice cooled enzyme buffer. The resulting mixture was then subjected to centrifugation at 12,000 g for 10 min at 4 °C. The supernatant obtained after centrifugation was used for determining the enzyme activity. The enzyme activities of APX, CAT, SOD, and POD were analyzed using different methods. APX was analyzed by measuring the decrease in optical density at A_{290}. CAT was analyzed using the ultraviolet absorption method, while nitroblue

tetrazolium NBT and guaiacol methods were used to analyze SOD and POD, respectively [33, 34]. To conduct ascorbate and glutathione content assays, a leaf sample of about 0.1 g was ground into a fine powder using liquid nitrogen and 1 mL of 0.2 M HCl was used for extraction. After centrifugation at 12,000 g for 10 min at a temperature of 4 °C, 0.5 mL of supernatant was mixed with 100 µL of 0.2 M phosphate buffer (pH 5.6). The mixture was then neutralized with 0.2 M NaOH to achieve a pH of 4–5. The extracts were neutralized and spectrophotometric assays were used to measure various compounds, including ascorbic acid (ASA), dehydroascorbic acid (DHA), glutathione (GSH), ascorbic acid/dehydroascorbate (AsA/DHA), glutathione disulfide (GSSG), and glutathione/oxidized glutathione (GSH/GSSG), following previously established methods [35].

Statistical analyses

Statistical analysis was performed using (Excel 2010; Microsoft Office 2010, Microsoft Corp., USA. Graphs were drawn using GraphPad Prism 5.0 (GraphPad Software, Inc., USA). Tukey's post-hoc tests was used to determine which means differed significantly with P-values (*$P<0.05$; to ***$P<0.01$). RT-qPCR data were normalized to a normal distribution as previously described by [36].

Results

Identification, characteristics and structural analysis of GhCDPK gene family

A total of 48 *GhCDPK*s were identified and classified as *GhCDPK1* to *GhCDPK48*, grouped into three main clusters (Fig. S1A). All 48 putative CDPK genes were characterized using ExPASy software. The analysis included determination of the corresponding amino acid numbers, pI, molecular weight, number of exons, subcellular location, and respective EF-hands (Table 1). Based on the predicted gene biochemical properties, the amino acid lengths of GhCDPK proteins ranged from 487 to 655 amino acids. The molecular weight (MW) of these proteins ranged from 54.63 kD to 73.42 kD, and their isoelectric point (PI) varied from 5.06 to 6.96 (Table 1). Most of the *GhCDPK* genes exhibited 3–4 EF-hand motifs, whereas *GhCDPK33*, *GhCDPK40*, *GhCDPK41*, and *GhCDPK42* contain only 2 EF-hand motifs (Table 1). Subsequent analysis revealed that 14 members possess potential N-myristoylation sites, including *GhCDPK16*, *17*, *18*, *20*, *21*, *22*, *24*, *35*, *37*, *39*, *43*, *44*, and *48*, while the remaining GhCDPK proteins were predicted to be non-myristoylated (Table 1). Based on subcellular localization prediction, all 48 *GhCDPK* genes are located in the nucleus (Table 1). Further results from the MEME software revealed 15 conserved motifs according to the ascending E-value of the alignment (Fig. 1B). In addition, motif 1–12 was present in all target *GhCDPK* genes, with the exception of *GhCDPK44*. Motif 13 was distributed in both subfamilies II and III and partially in subfamily I. The motif 14 was unique to subfamily I, whereas the motif 15 was present in subfamilies I and II but not in subfamily III (Fig. 2B). These findings show that the *GhCDPK* genes were both specific and conserved throughout evolution. Additionally, the differences in gene structure and conserved motifs indicate the relative conservation of the *GhCDPK* gene family during evolution and the diversity needed to adapt to the environment. The GhCDPK exon-intron structures showed that the intron numbers ranged from 6 to 7, while the exon numbers ranged from 7 to 9 (Fig. 1C).

Phylogenetic relationships and divergence of cotton CDPK proteins

The conserved protein sequences of the *GhCDPK* and *AtCDPK*, *ZmCDPK*, and *OsCDPK* genes were used to build the phylogenetic tree (Fig. 1). Based on the similar classified results from *Arabidopsis* CDPKs classification, four distinct groups were identified. Among them, the *GhCDPK* gene family was primarily distributed in groups I, II, and III, with 24, 18, and 6 representative genes, respectively, whereas group IV contained no *GhCDPK* gene (Fig. 1). Moreover, group I had 10, 15, and 11 CDPKs of *A. thaliana*, *Z. mays*, and *O. sativa*, respectively. Group II showed 13, 11, and 8 CDPKs; group III revealed a similar number of CDPK representative genes; and group IV showed 3, 6, and 3 CDPK genes of *AtCDPK*, *ZmCDPK*, and *OsCDPK*, respectively (Fig. 1).

Chromosomal localization and gene-duplication analysis of *GhCDPK*s

To understand gene evolution of the GhCDPK family, the chromosome localization of CDPK genes was analyzed using MapInspect software. Based on the results from Fig. 2A, *GhCDPK* genes were distributed on eighteen chromosomes, namely, At2, At3, At4, At6, At8, At9, At11, At12, At13, Dt13, Dt1, Dt2, Dt5, Dt6, Dt8, Dt9, Dt11, and Dt12 (Fig. 2A). In addition, most *GhCDPK* genes were distributed on the chromosome arms, with a few genes, including *GhCDPK4*, *GhCDPK7*, *GhCDPK5*, and *GhCDPK43*, located in the heterochromatin regions around the centromeric repeats. The chromosome Dt1 contained the largest number of CDPK genes, followed by chromosomes (At6, Dt6, and Dt9) and chromosomes (At8, Dt12, and Dt13) having 5, 4, and 3 chromosomes, respectively. Two chromosomes were located on At3, At9, At13, Dt8, and Dt5, while a single chromosome was found on At2, At4, At11, Dt2, and Dt11 chromosomes (Fig. 2A). Moreover, for the evolutionary relationship among GhCDPK members, the (Ks), (Ka), and Ka/Ks ratio values for each duplication event

Table 1 Characteristics of calcium-dependent protein kinases (CDPKs) in cotton

Gene name	Gene ID	Chr	Amino acid	MW (kDa)	PI	EF hands	*N*-terminal aa	*N*-myristoylation	Subcellular localization
GhCDPK1	CotAD_21360	At11	587	65.54	5.41	4	MGNTCVG	No	Nucleus
GhCDPK2	CotAD_33841	sca	573	64.03	5.87	3	MGNTCVG	No	Nucleus
GhCDPK3	CotAD_45432	Dt1	579	64.64	5.77	4	MGNTCVG	No	Nucleus
GhCDPK4	CotAD_53506	At12	605	67.32	5.66	4	MGNACAG	No	Nucleus
GhCDPK5	CotAD_34786	At9	540	60.67	6.10	4	MNKKIAG	No	Nucleus
GhCDPK6	CotAD_05939	Dt5	508	56.84	5.48	4	MNNQSSS	No	Nucleus
GhCDPK7	CotAD_36560	At3	511	57.14	5.48	4	MNNQSSS	No	Nucleus
GhCDPK8	CotAD_66485	sca	568	63.62	5.78	4	MGNTCRG	No	Nucleus
GhCDPK9	CotAD_13019	At8	607	67.88	5.76	3	MGNTCRG	No	Nucleus
GhCDPK10	CotAD_28390	Dt12	552	61.94	5.26	4	MGNTCRG	No	Nucleus
GhCDPK11	CotAD_50659	Dt2	648	71.66	5.32	4	MGNVCAT	No	Nucleus
GhCDPK12	CotAD_17127	At6	610	68.28	5.16	4	MGNNCFK	No	Nucleus
GhCDPK13	CotAD_12120	Dt13	487	54.63	5.06	4	MRRAIDH	No	Nucleus
GhCDPK14	CotAD_33393	At13	523	58.56	6.51	3	MGNTCLR	No	Nucleus
GhCDPK15	CotAD_12430	At9	532	59.52	5.38	4	MGNLCSR	No	Nucleus
GhCDPK16	CotAD_47701	Dt8	534	60.25	5.98	3	MGNCNSQ	Yes	Nucleus
GhCDPK17	CotAD_70650	sca	538	60.51	5.28	4	MGNCCSR	Yes	Nucleus
GhCDPK18	CotAD_16448	Dt1	513	57.31	5.27	4	MGNCCSR	Yes	Nucleus
GhCDPK19	CotAD_65954	At3	519	58.60	5.62	3	MGNCNGL	No	Nucleus
GhCDPK20	CotAD_49677	At6	523	58.55	5.69	4	MGNCCSC	Yes	Nucleus
GhCDPK21	CotAD_13649	Dt6	524	58.57	5.44	4	MGNCCSC	Yes	Nucleus
GhCDPK22	CotAD_41076	Dt9	524	58.82	5.98	4	MGGCLTK	Yes	Nucleus
GhCDPK23	CotAD_54795	sca	527	58.76	5.84	4	MGNCCTR	No	Nucleus
GhCDPK24	CotAD_73088	sca	537	60.46	6.14	4	MGSCLTK	Yes	Nucleus
GhCDPK25	CotAD_26791	Dt11	583	64.87	5.40	4	MGNTCVG	No	Nucleus
GhCDPK26	CotAD_48046	Dt12	600	66.47	5.48	4	MGNVCAT	No	Nucleus
GhCDPK27	CotAD_42895	Dt12	593	65.99	5.44	4	MGNACAG	No	Nucleus
GhCDPK28	CotAD_56181	Dt5	568	63.54	5.72	4	MGNTCRG	No	Nucleus
GhCDPK29	CotAD_33390	At13	487	54.62	5.06	4	MRRAIDH	No	Nucleus
GhCDPK30	CotAD_31563	Dt6	610	68.19	5.13	4	MGNNCFK	No	Nucleus
GhCDPK31	CotAD_34973	At8	655	73.42	6.04	3	MGNTCRG	No	Nucleus
GhCDPK32	CotAD_34966	At8	655	73.42	6.04	3	MGNTCRG	No	Nucleus
GhCDPK33	CotAD_12121	Dt13	570	63.63	5.93	2	MGNTCLG	No	Nucleus
GhCDPK34	CotAD_16744	Dt9	502	56.38	5.46	4	MNKKIA	No	Nucleus
GhCDPK35	CotAD_67913	Dt1	513	57.26	5.27	4	MGNCCTR	Yes	Nucleus
GhCDPK36	CotAD_04751	At4	527	58.72	6.09	4	MGNCCTR	No	Nucleus
GhCDPK37	CotAD_54317	Dt9	532	59.51	5.38	4	MGNLCSR	Yes	Nucleus
GhCDPK38	CotAD_07025	At2	537	60.54	6.06	4	MGTCLTK	Yes	Nucleus
GhCDPK39	CotAD_44026	Dt8	550	62.29	6.60	3	MGNCCAT	Yes	Nucleus
GhCDPK40	CotAD_20538	Dt6	531	60.23	6.32	2	MGNCCVT	No	Nucleus
GhCDPK41	CotAD_34534	Dt1	506	56.85	6.06	2	MGNCCAT	No	Nucleus
GhCDPK42	CotAD_16484	Dt1	529	59.39	6.96	2	MGNCCAT	No	Nucleus
GhCDPK43	CotAD_72552	Dt13	536	60.42	5.98	4	MGGCLTK	Yes	Nucleus
GhCDPK44	CotAD_48692	sca	531	59.69	5.37	4	MGNCCSR	Yes	Nucleus
GhCDPK45	CotAD_13610	Dt6	531	59.85	6.03	4	MGNCCAT	No	Nucleus
GhCDPK46	CotAD_20042	At6	531	59.86	6.17	4	MGNCCAT	No	Nucleus
GhCDPK47	CotAD_13386	Dt9	517	58.35	5.69	4	MGICQSL	No	Nucleus
GhCDPK48	CotAD_39468	sca	526	59.24	5.98	4	MGLCQSL	Yes	Nucleus

were calculated (Table S1). The Ka values ranged from 0.002 to 3.366, while the Ks values ranged from 0.026 to 3.104 (Table S1). The Ka/Ks ratio of paralogous pairs including *GhCDPK4/27*, *GhCDPK5/34*, *GhCDPK31/32*, *GhCDPK47/48*, *GhCDPK16/19*, *GhCDPK17/44*, and *GhCDPK41/42* segmental duplication was more than one, suggesting that this gene pair underwent positive selection while the other pairs of segmental duplications

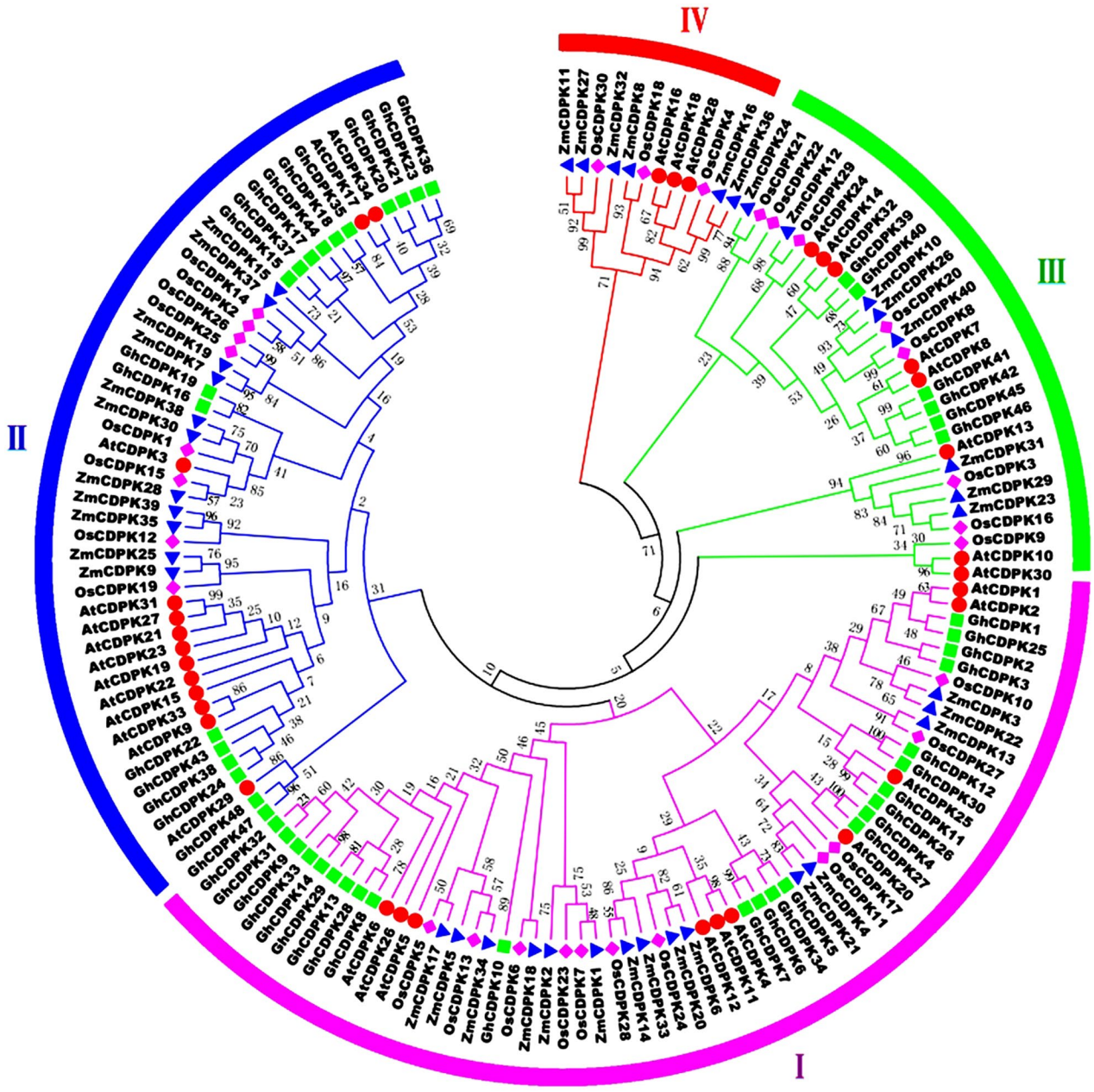

Fig. 1 Phylogenetic tree of CDPK proteins in *G.hirsutum*, *A.thaliana*, *Z.mays* and *O.sativa*. The phylogenetic tree was derived using the MEGA6.0 software, neighboring grouping method with a bootstrapping value of 1000 replicates. Species abbreviations are listed as follows: Gh: cotton; At: Arabidopsis; Os: rice; Zm: maize

had Ka/Ks < 1, indicating a negative selection during evolution (Fig. 2B; Table S1). Further analysis was necessary to determine the GhCDPK family's evolution and development. To ascertain the degree of collinearity among CDPK genes, we examined the genomes of maize, cotton, and *Arabidopsis* (Fig. 2C). Findings showed that there were 25 homologous gene pairs between the *AtCDPK* and *GhCDPK* genes, and 3 gene pairs between *ZmCDPK* and *GhCDPK* (Fig. 2C). The cotton CDPK gene shared more homology with dicotyledons than monocots, implying that the cotton and *Arabidopsis* CDPK families descended from a common ancestor.

Analysis of cis-acting elements of CDPK promoter

The cisregulatory elements of *GhCDPK* in the upstream sequences (~2000 bp) of their promoters linked to phytohormone signaling, plant growth and development, and response to biotic and abiotic stress were examined using the PlantCARE service online tool (Fig. 3; Additional file 1). Plant growth regulatory elements,

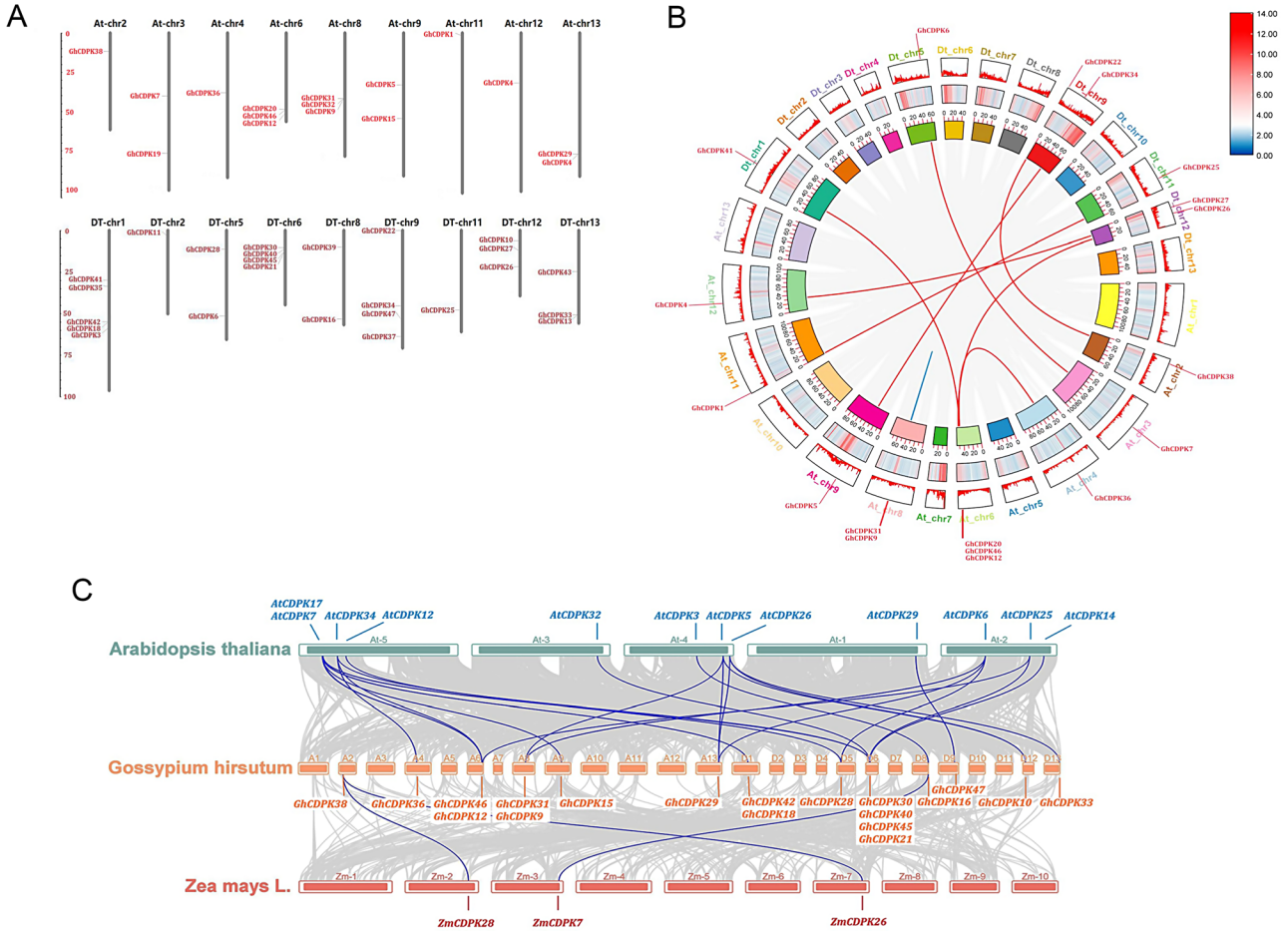

Fig. 2 Chromosomal localization, gene duplication, and collinearity analysis of the *GhCDPKs*. **A** designated *GhCDPK* gene locations on the cotton genome. **B** Fragment duplication analysis of the CDPK gene family in *G. hirsutum*. The red lines indicate duplicated CDPK gene pairs. **C** Collinearity analysis of the CDPK gene family in cotton, *Arabidopsis*, and *Zea mays*

including light responsiveness, endosperm expression responsiveness, circadian responsiveness, and flavonoid biosynthetic responsiveness, were predicted. The highest number of cisregulatory elements involved in stress, phytohormone signaling, and plant growth and development were found in group I *GhCDPK* genes (*GhCDPK11*, *26*, *30*, *27*, *6*, *7*, *32*, *9*, *8*, and *28*) and group II *GhCDPK* genes (*GhCDPK47*, *48*, *16*, *19*, *17*, and *44*) (Fig. 3B). Recorded plant growth and development elements were G-Box (38%), TCT-motif (12%), AE-Box (9%), O2-Site (7%), and CAT-Box (7%) (Fig. 3C). In addition, ABREs (30%), CGTCA-motif (18%), TGACG motifs (18%), and TGA elements (9%), and other phytohormone signaling elements, were also widely distributed in the *GhCDPK* gene promoter (Fig. 3D). Furthermore, stress response regulation elements for anaerobic responsiveness, defense and stress responsiveness, drought responsiveness, and low temperature responsiveness were found in the *GhCDPK* genes. Elements such as ARE (58%), TC-rich repeats (14%), LTR (8%), and MBS (10%) were the most abundant (Fig. 3E).

Predicted TF binding site analysis

TFBDS in CDPK genes were predicted. As displayed in Fig. 4, a total of 26 different TFs were observed in the GhCDPK family, with their length ranging from 7 to 29 bp. (Fig. 4; Additional file 2). Among them, the ethylene responsive transcription factor (ERFs) biding site constituted 60.09% of target sites in the GhCDPK family. Moreover, TFBDS, including *LBD*, *C2H2*, and *MYB*, were found to have a high interaction score with the GhCDPK gene family, indicating that a strong interaction might exist between TFs and the GhCDPK family proteins (Fig. 4). Although stress-responsive sites including *ERF*, *MYB*, *NAC*, *TCP*, *Bzip*, and *WRKY* were found in high quantity on target genes, hormone-related binding sites such as *AP2*, *ARF*, *bHLH*, and reproductive growth sites including *ARR*, *MIKC_MADS*, *G2-like*, and *TALE* were also recorded, suggesting that the GhCDPK family not only plays vital roles in the response to stress but may also perform some important functions in the hormone transduction and reproductive growth processes (Fig. 4).

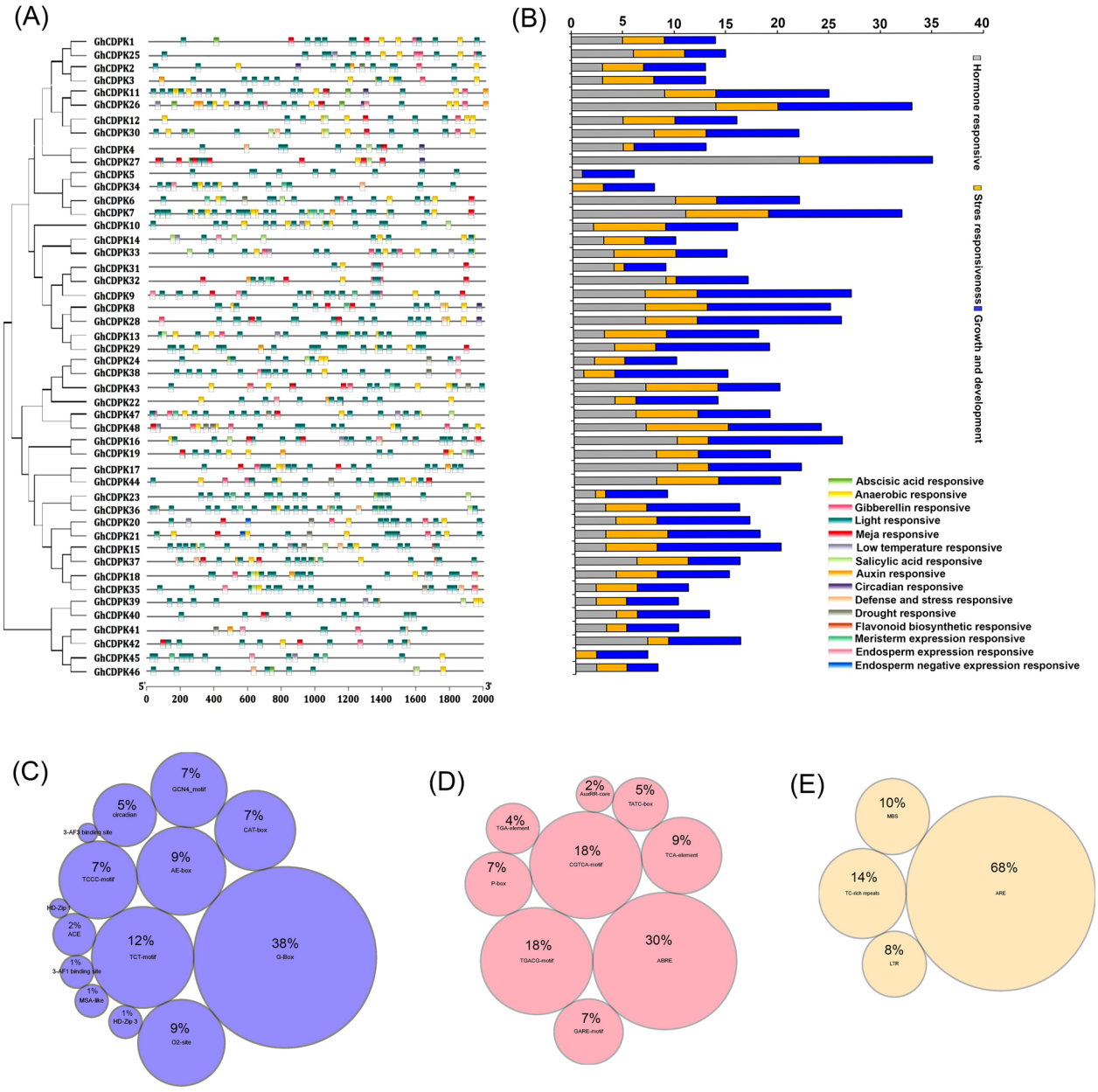

Fig. 3 Cis-element prediction in the 2000 bp region upstream of *GhCDPKs*. **A** Different types of predicted cis regulatory elements in *GhCDPK* promoters. **B** The number of cis-regulatory elements involved in phytohormone signaling, plant growth and development, and abiotic and biotic stress. **C-E** The type and quantity of the *GhCDPK* cis elements responsive to plant growth and development, phytohormone signaling, and biotic and abiotic stress, respectively

Heat stress responsive expression pattern of the GhCDPK family

To deeply verify the roles of the GhCDPK family in response to heat stress, the expression levels of all 48 target genes were examined under 0, 1, 2, 4, 8, and 12 h of stress treatment (Fig. 5). Numerous *GhCDPK* genes exhibit increased expression in response to increased stress treatment, as seen in Fig. 5. For instance, following one and two hours of heat stress treatment, the expression patterns of *GhCDPK45*, *GhCDPK40*, *GhCDPK37*, *GhCDPK38*, and *GhCDPK10* were responsively high; however, this response decreased as treatment levels increased (Fig. 5). After 4 h of heat stress treatment, target genes including *GhCDPK45*, *GhCDPK37*, *GhCDPK15*, *GhCDPK18*, *GhCDPK36*, *GhCDPK23*, *GhCDPK19*, *GhCDPK16*, *GhCDPK28*, *GhCDPK27*, *GhCDPK4*, and *GhCDPK2* were highly upregulated, whereas *GhCDPK45*, *GhCDPK15*,

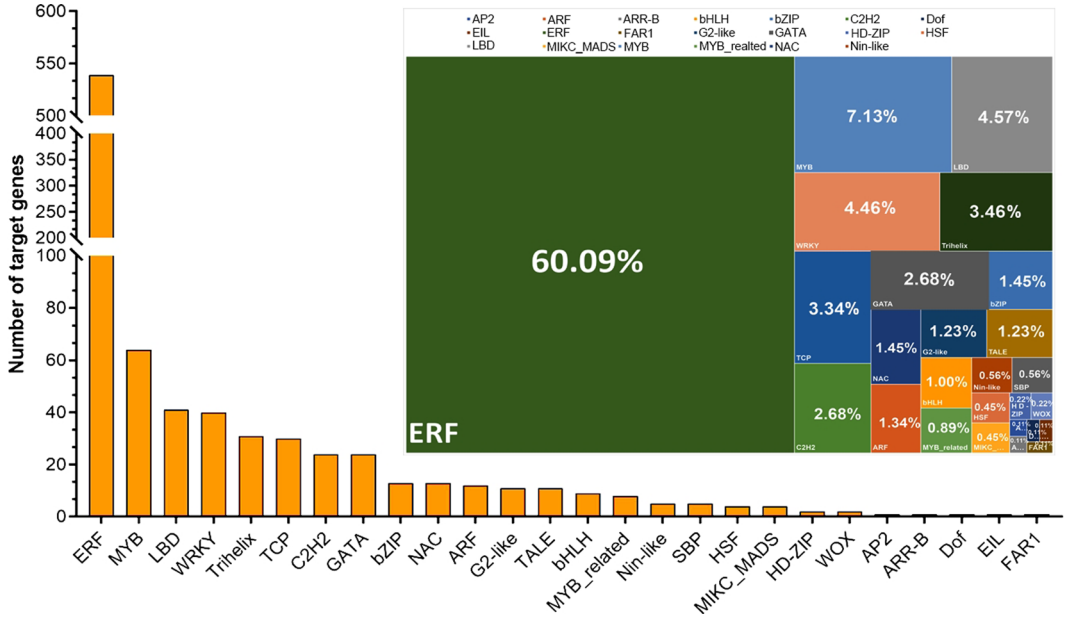

Fig. 4 Predicted transcription factor binding sites of *GhCDPK* members in the cotton genome. The tree map chart showed the percentage of the various transcription factors in each *GhCDPK* family gene

GhCDPK18, *GhCDPK17*, *GhCDPK19*, *GhCDPK16*, and *GhCDPK27* were significantly expressed after 8 h of stress treatment (Fig. 5). After 12 h of stress treatment, *GhCDPK15*, *GhCDPK16*, and *GhCDPK19* were highly expressed. However, significant expressions were observed in *GhCDPK16* and *GhCDPK19* (Fig. 5). Contrarily, the expression levels of *GhCDPK46*, *GhCDPK14*, *GhCDPK46*, *GhCDPK1*, *GhCDPK25*, *GhCDPK26*, *GhCDPK30*, *GhCDPK48* and *GhCDPK47* showed no significant responses to heat stress treatments.

Predicted functional interaction network of GhCPK16 proteins

The expression pattern of the *GhCDPK16* and *GhCDPK19* genes validates a possible role in heat stress responses. However, the interacting role with other proteins remains unclear. Thus, an interaction analysis was carried out based on *GhCDPK16* to investigate the interaction patterns in *A. thaliana* and *G. hirsutum* genome proteins, was required (Fig. 6). The results showed that various ROS generating protein genes in the *A. thaliana* genome interacted with *GhCDPK16* (Fig. 6A) such as *RbohD*, *RbohB* and *RbohF*. In addition, the guard cell S-type anion channel (*SLAC1*), leucine-rich repeat receptor-like protein kinases (*LRR*), Ricin B-like lectin (*EULS3*) and calcineurin B-like (*CBL1* and *9*) proteins were found to interact with the putative GhCDPK protein in reference to *A. thaliana* genome (Fig. 6A). In relation to *G. hirsutum* genome proteins, predicted results showed that *GhCDPK16* similarly associated with several respiratory oxidase homolog proteins (RBOH), which may promote ROS content during stress (Fig. 6B). The analysis showed that *GhCDPK16* genes interact with three different groups of proteins. The cluster I proteins comprises calmodulin-like (CML-like), calcium-binding protein (*CML45* and *CML30*), and protein time for coffee-like (Fig. 6B). Furthermore, various RBOH-generating proteins were found to interact with the target gene, grouped as cluster IIAB. In this group, several respiratory oxidase homolog proteins, including *RbohA-like*, *RbohB-like*, *RbohC-like*, *RbohC-like*, *RbohD-like*, *RbohE-like*, and *RbohF-like*, were found as predicted interactors (Fig. 6B). Other proteins including *WRKY33*, LRR, *SLAC1-like*, aquaporin (*NIP2-1-like*), and spastin-like also interacted with the target protein. Furthermore, the cluster gene group III included heat stress transcription factor A-3-like (*HSFA-like*) and N-(5-phosphoribosyl) anthranilate isomerase-1 chloroplastic-like (*TSB1*) protein genes (Fig. 6B). This indicated that the *GhCDPK16* gene may have a role in heat stress tolerance by regulating ROS generation protein genes.

GhCDPK16 expression improves thermotolerance in transgenic plants

Transgenic cotton and *Arabidopsis* lines were subjected to high temperature stress to examine the function of *GhCDPK16*. As seen in Fig. 7A and B, transient overexpression and cas9 knockout techniques were employed in this study. The observed phenotype was leaf curling; however, the heat stress effect intensity was significantly higher in wild-type and Cas9 knockout plants than in *GhCDPK16*-OE lines (Fig. 7C). Furthermore, in comparison to the wild-type and the cas9 lines, the overexpressed lines had higher levels of *GhCDPK16* expression

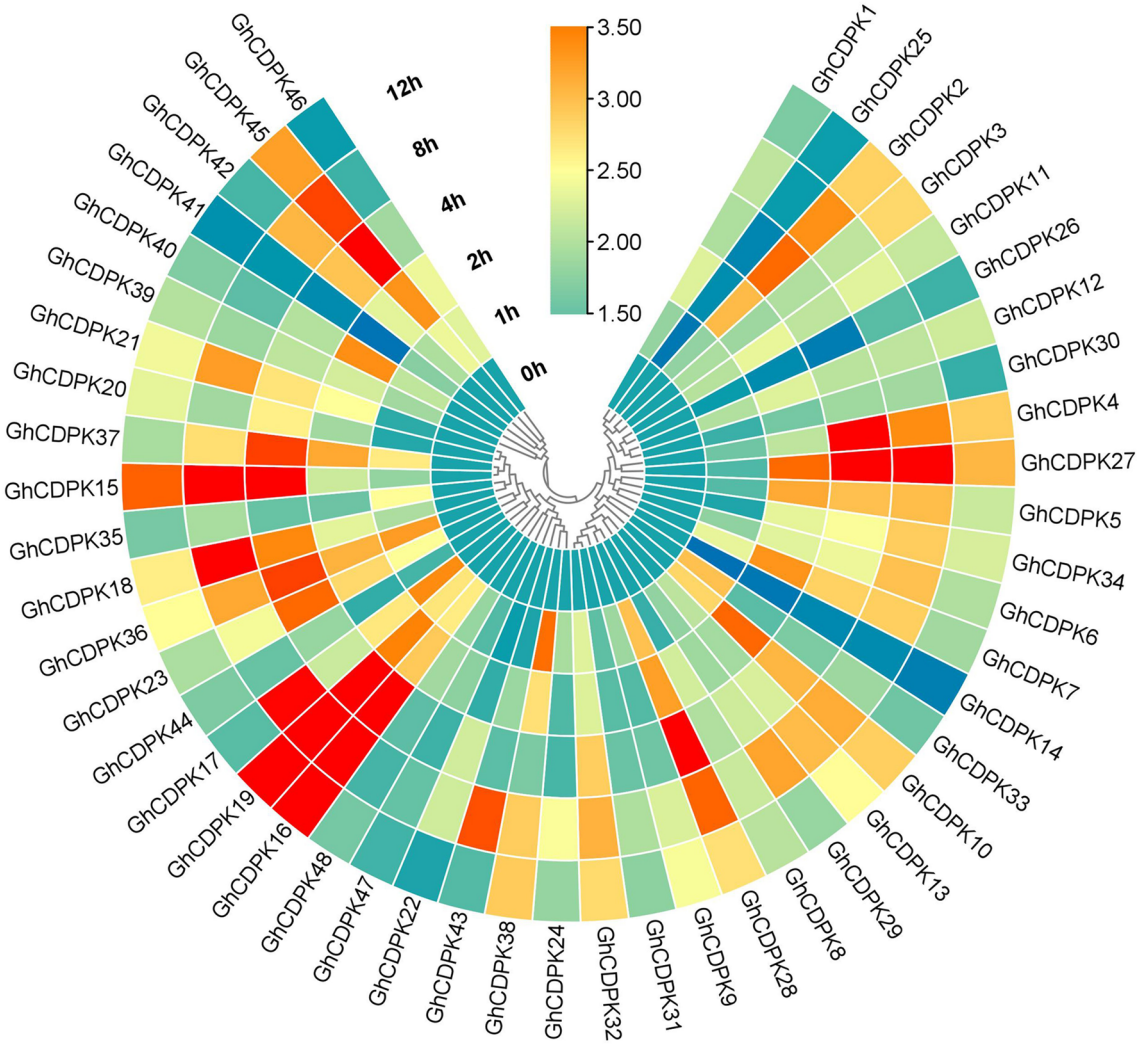

Fig. 5 The expression profiles and functional network analysis of *GhCDPK* proteins. Circular heatmap of *GhCDPK* family genes at different heat stress time points

(Fig. 7D). For further validation, the expression levels of heat-inducible genes *GhHSP70*, *GhHSP17.3*, *GhGR1* were dramatically increased in overexpressed cotton lines (Fig. 7E), possibly contributing to cotton's thermotolerance. In *Arabidopsis*, thermotoleance validation was conducted at different growth stages. For seed germination responses after an hour of stress treatment 5 days of recovery, results showed an increase in germination rate in *GhCDPK16*-ox transgenic lines compared to the wild type (Fig. 8A and B). In addition, line 4 and line 5 showed increased germination rates compared to line 3 (Fig. 8B). At the seedling stage of 7 days and 2 h of heat stress, the *Arabidopsis* line exhibits more significant signs of tolerance to heat stress than the wild type. Moreover, transgenic *GhCDPK16* seedlings line 3 and line 5 showed a significant survival rate in comparison to the wild-type (Fig. 8C and D). After 4 weeks of plant growth and high temperature treatments at 45 °C for 24 h, the wild-type leaves showed severe wrinkling and drying, while the leaves of the overexpression lines showed fewer wrinkling compared to the WT (Fig. 8E).

GhCDPK16 thermotolerance hinders ROS accumulation

To investigate the expectations of ROS accumulation in transgenic and wild-type plants, the concentrations of H_2O_2 and MDA were evaluated in transgenic cotton following a 42 °C stress. To be precise, H_2O_2 content in overexpressed cotton leaves decreased by 0.16 folds compared to the control, whereas *GhCDPK16* knockout lines showed a significant increase of 0.28 folds in comparison with the control under heat stress conditions. Contrarily, H_2O_2 levels under no stress were negligible ($P>0.05$) (Fig. 9A). Likewise, MDA content in *GhCDPK16*-OE cotton leaves greatly decreased by 0.36 folds, contrary to an enhancement of 0.2 folds in knockout lines, respectively (Fig. 9B). Similarly, the accumulation of H_2O_2 and

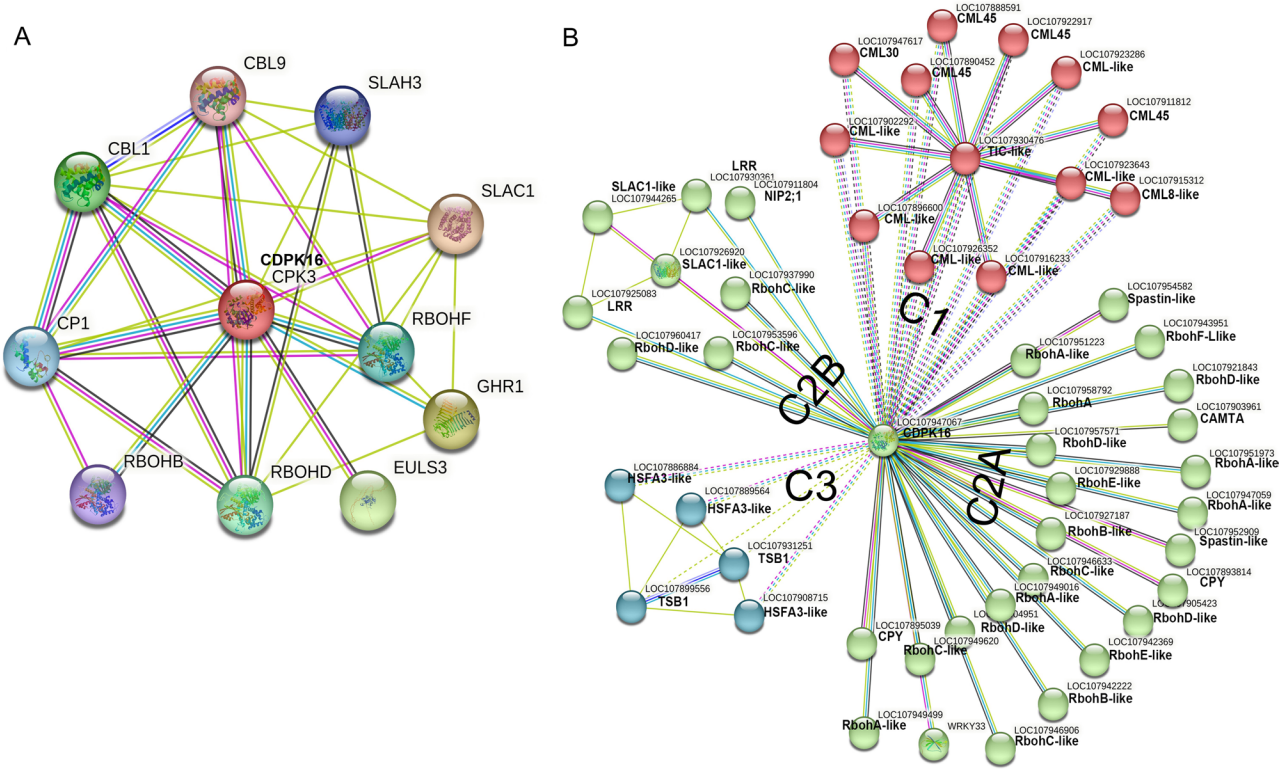

Fig. 6 Predicted interaction networks based on the orthologs in *A. thaliana* and *G. hirsutum*. **A***GhCDPK16* protein interaction in A. thaliana; the colored nodes denote query proteins and the first shell of interactors; the white nodes are the second shell of interactors. Light blue, pink, green, red, blue, black, and purple edges represent known interactions; experimentally known interactions; predicted gene neighborhoods; predicted gene fusions; predicted gene co-occurrences; coexpression; and protein homology, respectively. **B***GhCDPK16* protein interaction in *G. hirsutum*: black, green, and blue lines indicate predicted co-expression, textmining and database interaction evidence. Different colored nodes indicate K-means clustering based on their centroids. The edges indicate both functional and physical protein associations

O_2^- were evaluated in *Arabidopsis* leaves using the DAB and NBT staining techniques. Under normal growth conditions, DAB and NBT results showed no significant difference between WT and transgenic *Arabidopsis*, whereas brown and blue staining increased significantly in WT leaves compared to transgenic plants after 2 h of heat stress (Fig. 10A and B), signifying the presence of a high ROS concentration. Staining intensity levels confirmed the concentration levels in plant leaves (Fig. 10C and D). Furthermore, the levels of H_2O_2 were quantified in leaf samples. As depicted in Fig. 10E, the H_2O_2 concentration under normal conditions showed no significant difference between the transgenic plants and the wild-type. However, H_2O_2 levels were lower in transgenic plants than in wild-type after high-temperature treatment (Fig. 10E). This indicates that ROS may have played a significant role in heat stress treatment.

Overexpression of *GhCDPK16* increases antioxidants protection under heat stress

Understanding the endogenous amounts of antioxidant compounds under *GhCDPK16* thermotolerance will be beneficial in this study in terms of lowered ROS component concentrations. To do so, major antioxidant enzyme levels, including APX, POD, SOD, CAT, ascorbate, and glutathione, were determined in both cotton and *Arabidopsis* wild-type and transgenic plants. The results showed no significant differences in antioxidant enzyme activities between transgenic plants and WT plants under normal growth conditions. Nonetheless, POD, CAT, APX, and SOD were significantly higher in *GhCDPK16*-OE transgenic cotton and *Arabidopsis* lines compared to the wild-type (Figs. 9C-F and 11A-D). Similar increasing trends were observed in ASA, GSH, GSH/GSSG, and ASA/DHA antioxidant concentration levels in the transgenic leaves, but ASA, GSH, GSH/GSSG, and ASA/DHA content under normal temperatures were higher than heat stress (Figs. 9G, I, J and K and 11E, G, I and J). Whereas antioxidant levels in *GhCDPK16*-OE leaves increased dramatically, *GhCDPK16*-knockout cotton leaves decreased significantly when compared to the control. Contrary to the above mentioned antioxidants, only DHA and GSSG showed a decreased in antioxidant levels in overexpressed lines when compared to the wild-type (Figs. 9H and L and 11F and H). Furthermore,

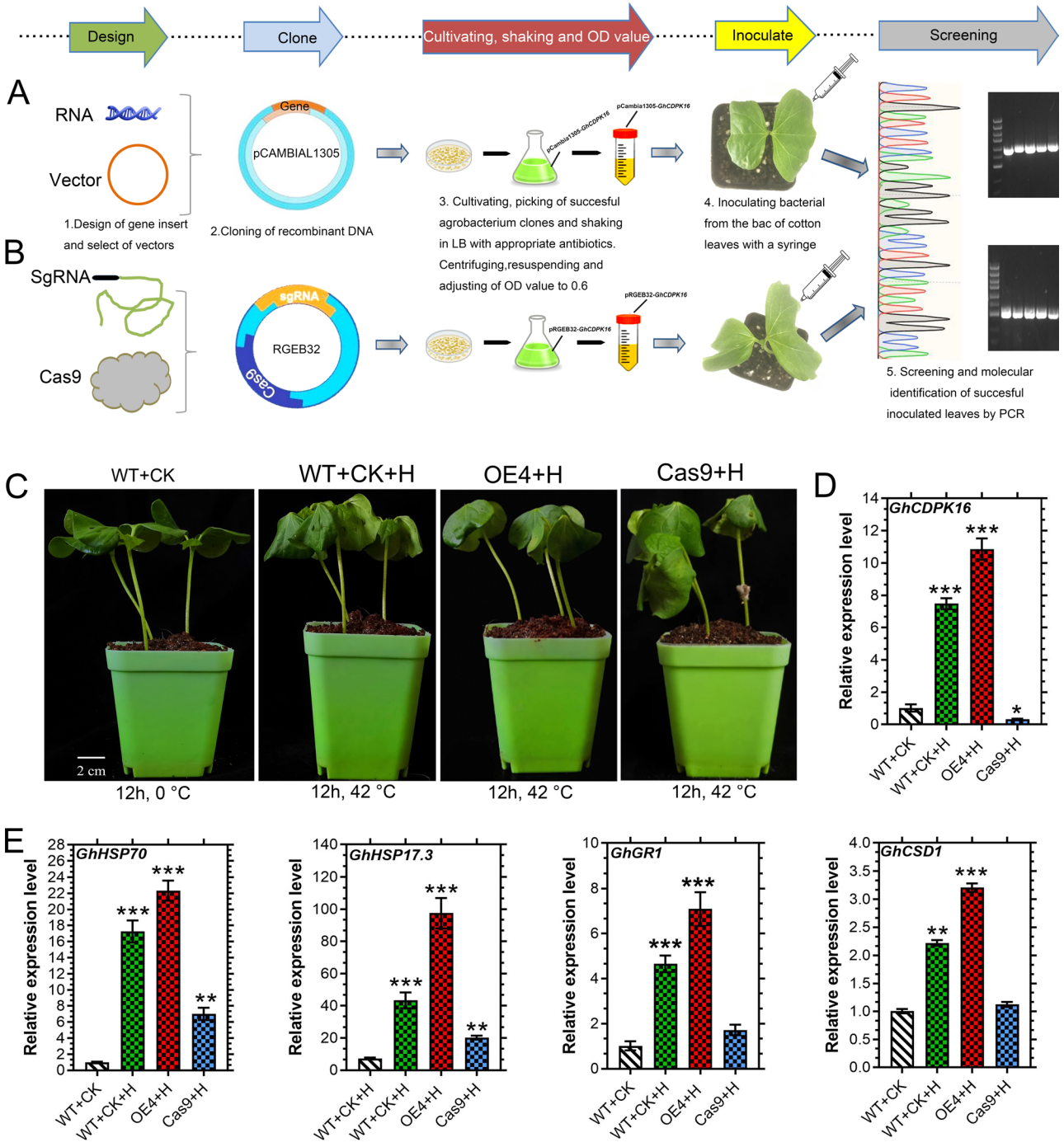

Fig. 7 Schematic views of transient expressions and CRISPR-Cas9 technology and thermotolerance assay in cotton transgenic lines. **A** Agrobacterium-mediated transient transfromation. **B** Agrobacterium-mediated CRISPR-Cas9 knockout transformation. **C** phenotype expression of cotton transgenic plants under heat stress. **D** The expression of GhCDPK16 in transient overexpression in CRISPR-cas9 knockout cotton plants. **E** Expresion analysis of heat-inducible genes in the transgenic plants. Asterisks * to *** represent significant differences ($P < 0.05$ to $P < 0.01$ two-way ANOVA with Tukey's HSD post hoc test), while no asterisks denote no significant differences

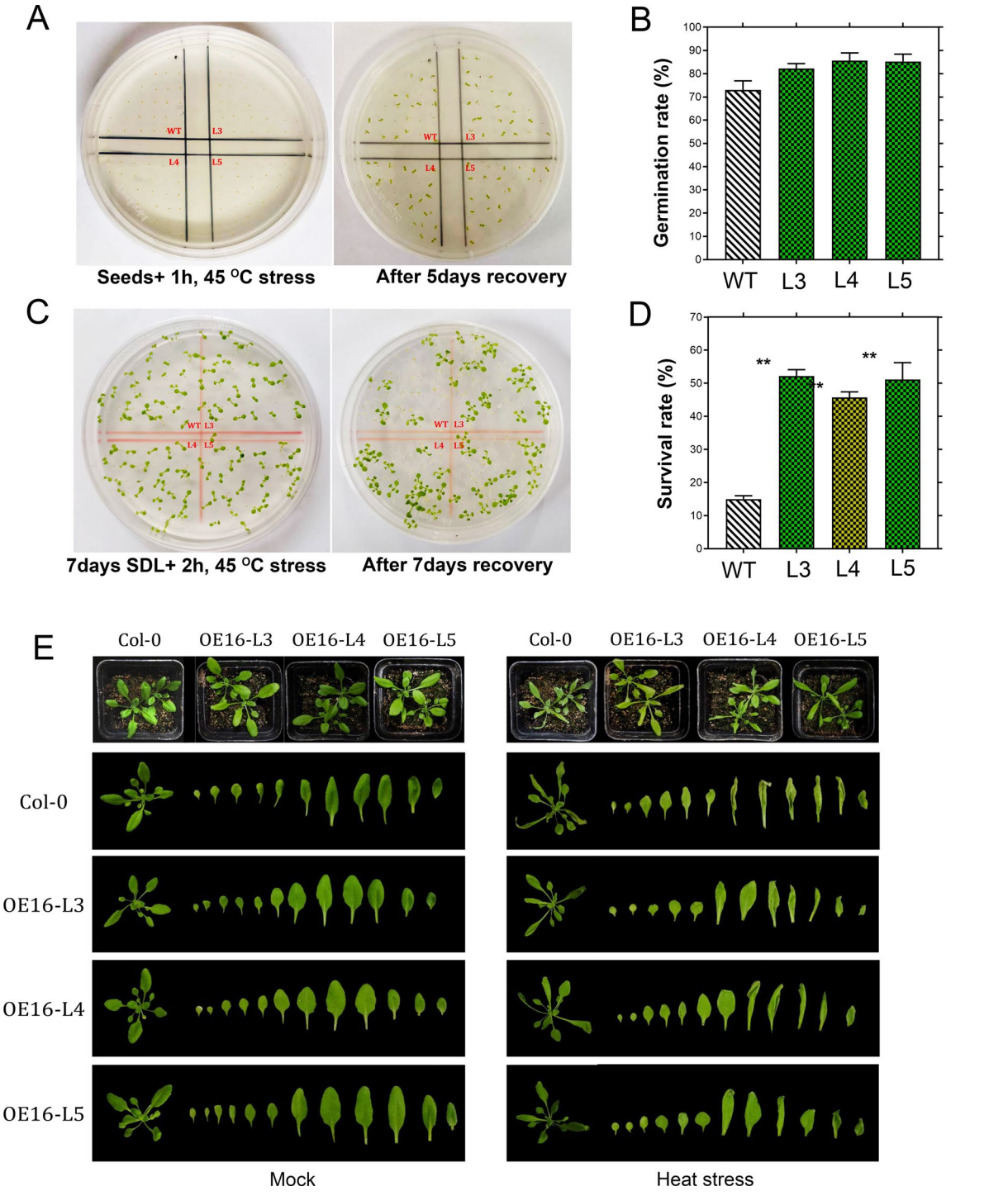

Fig. 8 Different growth stages of the *GhCDPK16* transgenic line and wild-type responses under heat stress treatments. **A** Seed germination response to heat stress and 5-day recovery after treatment. **B** Germination rate analysis. **C** Seven-day-old seedling responses to heat stress and 7 days of recovery after treatment. **D** Survival rate analysis. **E** Phenologic changes of 4-week-old plants under heat stress treatments. SDL denotes seedlings. Each data point represents the mean (with SD bar) of three replicates. Asterisks * to *** represent significant differences ($P < 0.05$ to $P < 0.01$ two-way ANOVA with Tukey's HSD post hoc test), while no asterisks denote no significant differences

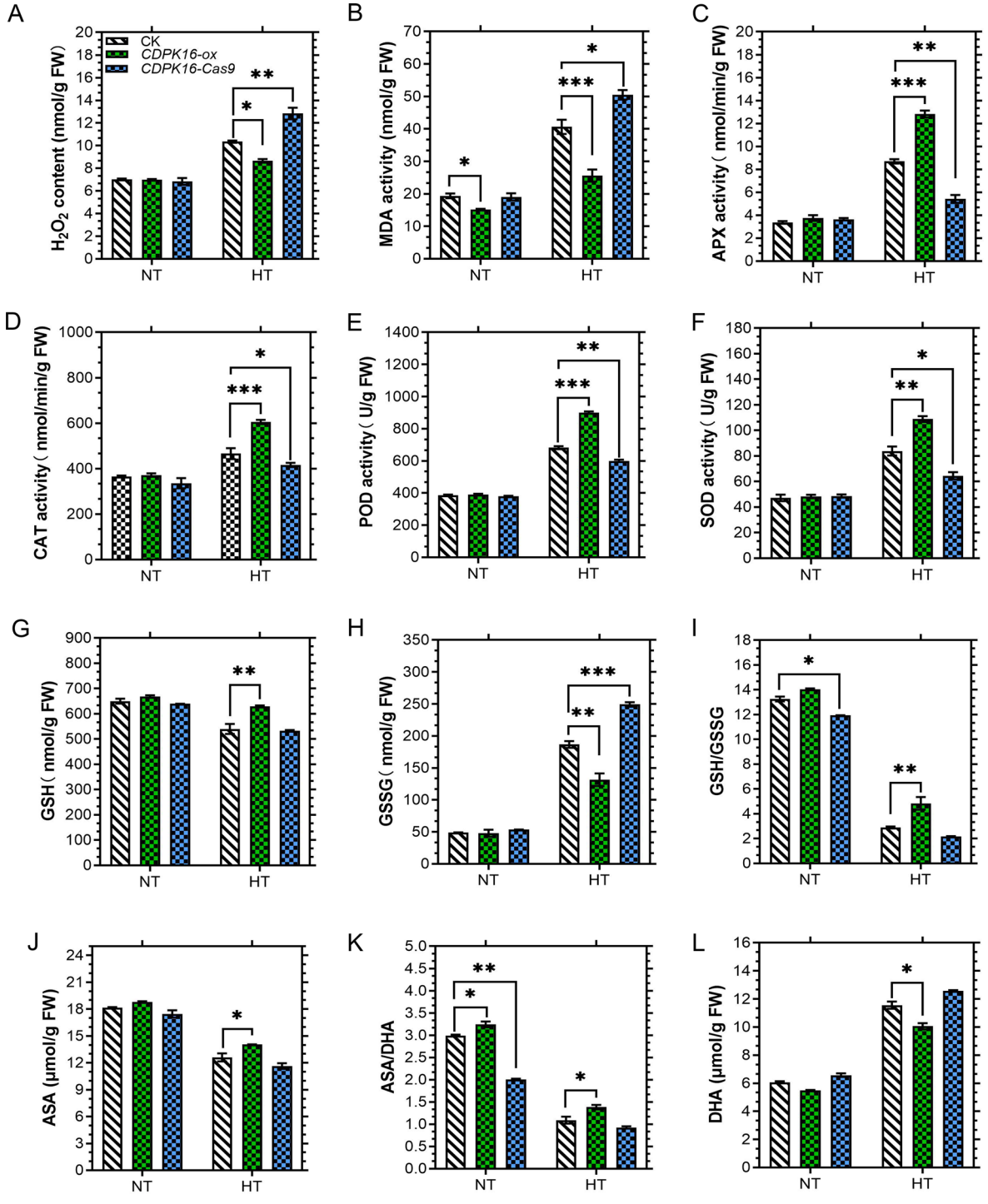

Fig. 9 Overexpression of *GhCDPK16* in cotton reduces ROS accumulation. A H_2O_2 content. B MDA content. C Ascorbate peroxidase (APX) activity. D Catalase (CAT) activity. E Peroxidase (POD) activity. F Superoxide dismutase (SOD) activity. G Glutathione (GSH) content. H Glutathione disulfide (GSSG) content. I Glutathione/oxidized glutathione (GSH/GSSG) content. J Ascorbate (ASA) content. K Ascorbic acid/dehydroascorbate (AsA/DHA) content. L Dehydroascorbate (DHA) content. Asterisks * to *** represent significant differences ($P < 0.05$ to $P < 0.01$ two-way ANOVA with Tukey's HSD post hoc test), while no asterisks denote no significant differences

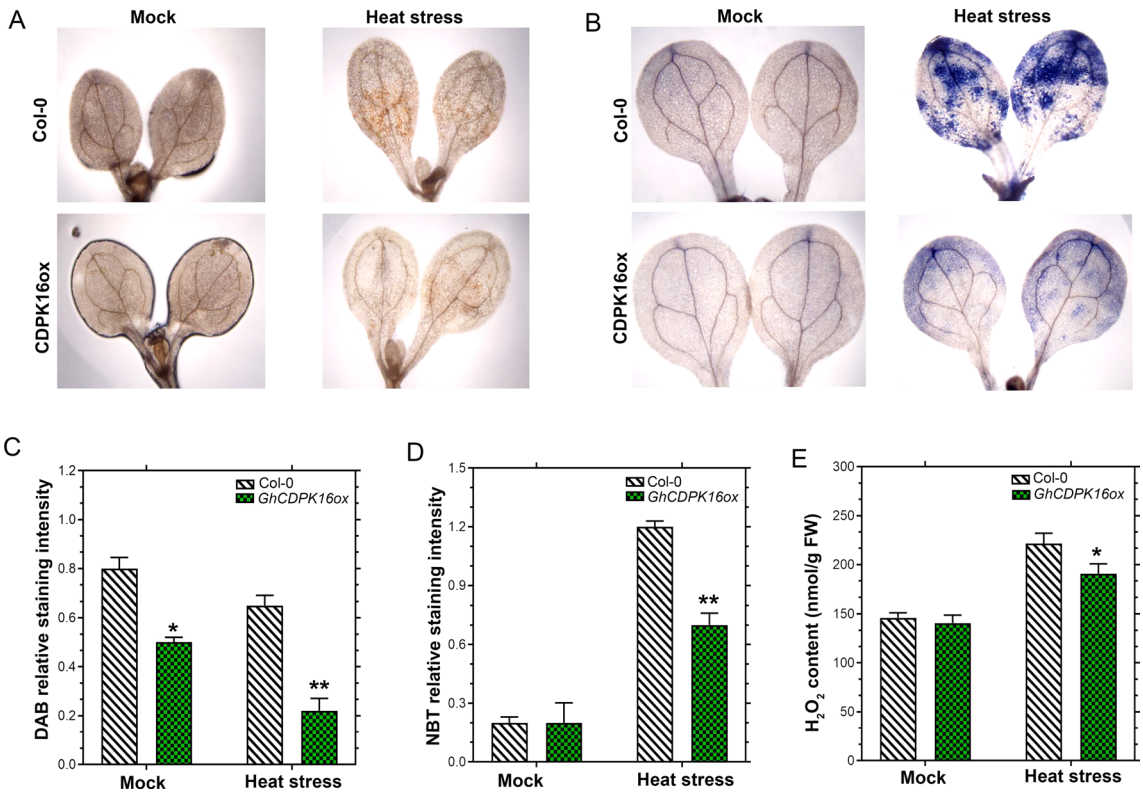

Fig. 10 Histochemical and H_2O_2 levels in *GhCDPK16* transgenic lines. **A** H_2O_2 quantity visualized by 3,3-diaminobenzidine (DAB) staining. **B** Superoxide anion radicals (O_2^-) quantity visualized by nitroblue tetrazolium (NBT). **C** and **D** staining intensity as determined with ImageJ software. **E** Quantification of H_2O_2 content. Asterisks * to *** represent significant differences ($P < 0.05$ to $P < 0.01$ two-way ANOVA with Tukey's HSD post hoc test), while no asterisks denote no significant differences

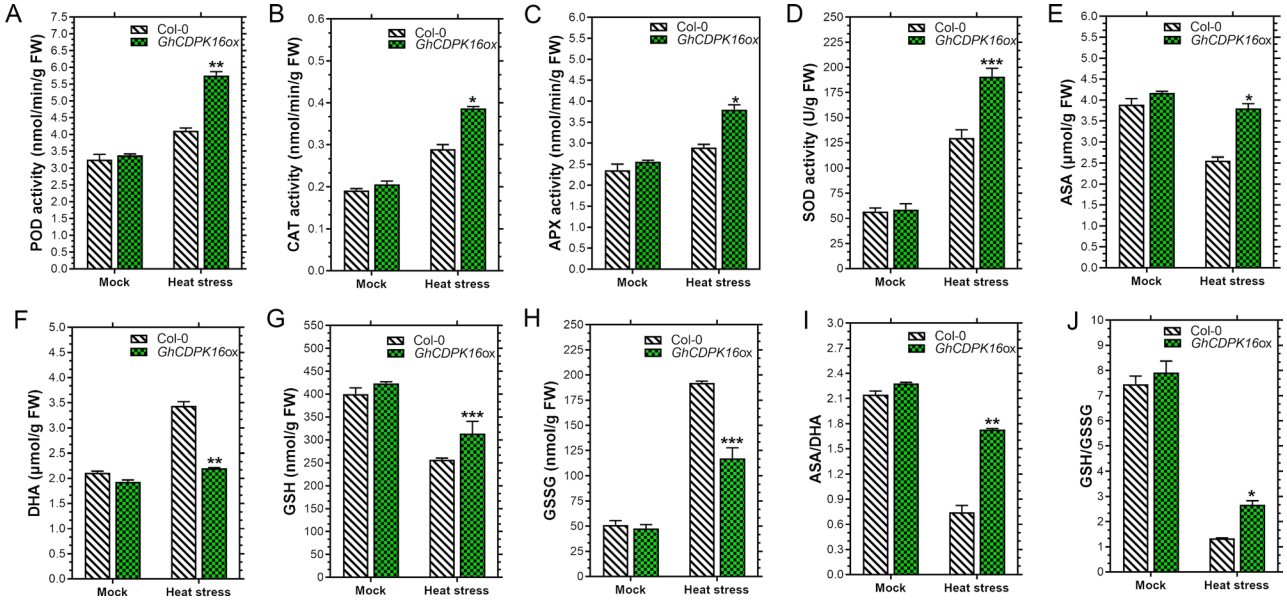

Fig. 11 Endogenous antioxidant enzyme activities in *GhCDPK16* transgenic and wild-type plants under heat stress. **A** Peroxidase (POD) activity. **B** Catalase (CAT) activity. **C** Ascorbate peroxidase (APX) activity. **D** Superoxide dismutase (SOD) activity. **E** Ascorbate (ASA) content. **F** Dehydroascorbate (DHA) content. **G** Glutathione (GSH) content. **H** Glutathione disulfide (GSSG) content. **I** Ascorbic acid/dehydroascorbate (AsA/DHA) content. **J** Glutathione/oxidized glutathione (GSH/GSSG) content. Each data point represents the mean (with SD bar) of three replicates. Asterisks * to *** represent significant differences ($P < 0.05$ to $P < 0.01$ two-way ANOVA with Tukey's HSD post hoc test), while no asterisks denote no significant differences

in cotton genotypes, *GhCDPK16*-Cas9 levels rose and *GhCDPK16*-ox antioxidant levels declined.

Discussion

The CDPK gene was first reported to be physiologically activated by calcium ions in pea shoot membranes [37]. After a considerable years of research, the CDPK gene family was found to comprise of a sizable multigene family of CPK proteins that are present in all plants species with additional functional role in stress tolerance [9, 11]. Over the past few years, the characterization and evolution of the CDPK genes in the cotton genome has been extensively explored. For example, 41 putative cotton CDPKs were identified in a diploid *Gossypium raimondi* [21, 38], eighty-four CDPK genes were identified in *G. barbadense*, and 96, 44, and 57 CDPKs were identified in *Gossypium hirsutum*, *Gossypium raimondii*, and *Gossypium arboretum* [39] respectively. In addition, the cotton CDPK genes have been reported to be functionally involved in both biotic and abiotic roles such as verticillium wilt resistance, drought stress, and positive regulators of salt stress [17, 39, 40]. However, to date, the abiotic functional role of the plant CDPK gene family in heat stress tolerance has not been well understood. The CDPK biochemical structure of the *Gossypium barbadense* cultivar showed encoded amino acid lengths ranging from 648 to 155 with molecular weights ranging from 17.99 kDa to 71.854 kDa and predicted isoelectric point ranges from 4.313 to 9.48 [24]. In *G. raimondii*, *G. arboretum*, and *G. hirsutum* CDPK proteins, amino acid length varied from 64 to 907 amino acids, the molecular weight (MW) ranged from 6.726 kDa to 101.033 kDa, and the isoelectric point (IP) ranged from 4.128 to 10.72 [39]. In the present study, the amino acid lengths of *GhCDPK* proteins ranged from 487 to 655, the molecular weight (MW) ranged from 54.63 kDa to 73.42 kDa, and the PI varied from 5.06 to 6.96 (Table 1).

The tree phylogeny studied among *GhCDPK* members clustered into 3 major groups, with reference to *A. thaliana*, *Z. mays*, and *O. sativa* (Fig. 1 and S1A). However, contrary to previous reports, the evolutionary relationships among *AtCDPKs*, *OsCDPKs*, *FaCDPKs*, and *GrCDPKs* revealed four classified groups, indicating a possible divergence during evolution [9, 38]. According to existing reports, *AtCDPK23* responds to drought and salt stresses, while *GhCDPK60* positively regulates drought stress [17, 41]. In addition, *AtCDPK7* and *AtCDPK8* cluster in the same subgroup with *GhCDPK60* [17]. In the present study, both *AtCDPK7* and *AtCDPK8* were present in a similar subgroup with *GhCDPK41*, *42*, *46*, and *46*, signifying a possible involvement in drought stress response. The expression profile of *GbCDPK24* revealed high responses after 24 h of heat stress [24]. Moreover, *AtCDPK17* and *AtCDPK34* were present in a similar group with *GbCDPK24* deducing a similar role under abiotic stress responses. In the present work, *AtCDPK17 and AtCDPK34* were similarly present in Group II. Additionally, the *ZmCDPK7* gene, known to function in heat stress tolerance [7] was present in a similar subgroup with the *GhCDPK* gene in group II. A genome-wide study in *Brachypodium distachyon* showed the expression patterns of heat-tolerant *BdCDPK* genes, including *BdCDPK24* and *BdCDPK10*. Moreover, in references to *AtCDPKs*, *BdCDPK24* was present in the same cluster as *AtCDPK34*, 17, and 3 [42]. In the study, *AtCDPK34*, 17, and 3 clustered together in *GhCDPK* genes in group II, but *AtCDPK3* was present in the same subgroup as *GhCDPK16/19* (Fig. 1). Thus, we speculated that group II *GhCDPK* genes may have a role in heat stress tolerance. Orthologous genes are thought to have similar biological functions. Therefore, the function of *GhCDPK* genes can be inferred from orthologous genes to provide a scientific theoretical basis for subsequent functional studies [24, 43].

A typical characteristic of a CDPK structure is thought to have an N-terminal domain, a junction domain, a calmodulin-like Ca^{2+} binding domain, a protein kinase domain, and an EF-hand domain [9]. The EF hand allows for calcium binding, and N-myristoylation terminal domains function as part of a primary signaling process that directs proteins to the cell membrane, cytoplasm, or nucleus [9, 44]. We found all CDPKs possessing an EF-hand and a kinase domain; also, 14 putative CDPK genes were observed to have the N-terminal domain, indicating the possibility of Ca^{2+} binding ability and signaling functions (Table 1). The subcellular locations of CDPKs are widely distributed throughout plant cells. The plasma membrane, cytoplasm, endoplasmic reticulum, nucleus, mitochondria, oily bodies, peroxisomes, chloroplasts, and the Golgi complex are already reported locations of CDPKs [45]. In the present study, all *GhCDPK* genes were localized in the nucleus (Table 1). The binding sites of cis-regulatory in the gene promoter sequences play a major role in regulating the expression of the genes and controlling the growth, development, and stress responses in plants [27, 46]. As a matter of fact, the structure of the promoter could suggest the possible functions and regulatory mechanisms of the genes [47]. The MYC promoter element was reported to be involved in drought, salt, and ABA stress responses during the plant's life cycle [48]. In addition, ABRE responded to drought and ABA through ABRE-binding proteins (AREBs) [49]. MYB is known to respond to drought, low temperatures, salt, ABA, and GA stress in plants [50]. Moreover, in *Morus atropurpurea Roxb*, an ABA response element (MBS, ABRE, and GARE-motif) was reported to positively respond to drought and salt stresses in *Morus atropurpurea* by interaction with *MaCDPK1* [48]. Consistent with the present

study, these mentioned promoters were among predicted cisregulatory analysis revealed to associate with *GhCDPKs* (Fig. 3). Stress-responsive promoter elements such as MBS, ARE, TC-rich repeats, LTR, and cis-regulatory elements involved in phytohormone pathways (ABA, GA, MeJA, and SA) were recorded, suggesting that GhCDPK could stress-responsively interact with plant hormones to defend against plant stress. Furthermore, the highest number of cis-elements was observed in *A. thaliana*, *Z. mays*, and *P. sativum*, implying multiple stress resistance pathways.

Gene expressions are usually controlled by sequence-specific DNA-binding proteins known as transcription factors. These factors recognize specific DNA sequences TFBSs and are thus targeted to specific genomic regions where they can recruit transcriptional co-factors and chromatin regulators to fine-tune spatio-temporal gene regulation [51]. Thus, the identification of TFBSs in genomic sequences is essential for understanding and predicting gene expression. In the present study, we examined the TFB sites of the *GhCDPK* genome sequence, revealing TFBS sites including *ERF*, *MYB*, *LBD*, *WRKY*, *Trihelix*, *TCP*, *NAC*, etc. (Fig. 4). The ethylene responsive transcription factor (ERF) was reported to regulate primary and secondary metabolism, growth, and developmental programs, as well as the tolerance of plants to various stresses, including heat stress [52, 53]. The *MYB* TF responds to various environmental stresses and plays a role in tolerance to high temperatures [54]. The *WRKY* TF family is known to be involved in high-temperature responses and can bind to the W-box cis-acting elements of target gene promoters, thereby regulating the expression of multiple types of target genes [55]. Moreover, the high number of *trihelix*, *TCP* and *NAC* biding sites indicates plant growth, development regulation, and stress response signaling in the *GhCDPK* genomic sequence [56–58].

The responsive gene expression patterns of all *GhCDPKs* were clearly presented in Fig. 5A. Among them, *GhCDPK16/19* genes were significantly responsive to increasing heat stress as stress time increased. These results suggest the involvement of *GhCDPK16/19* in tolerance to abiotic stress, especially heat stress tolerance. Moreover, the underlying biochemical mechanisms are still unknown. Therefore, using protein-protein interactions analysis will be essential towards understanding the mechanisms involved in *GhCDPK16* towards heat stress tolerance. The interaction network based on the co-expression analysis revealed that *GhCDPK16* is significantly associated with *RBOHs*, followed by *WRKY*, *LRRs*, *CBLs*, *SLAC1-like*, *HSFs*, and *CML*-related gene families (Fig. 5B). *RBOHs* are integral membrane proteins that convert superoxide anions into H_2O_2. The structure of *RBOHs* are made up of two calcium-binding EF hand motifs and multiple phosphorylation sites at their N-termini, enabling them to participate in the regulation of enzyme activity and regulate responses to abiotic stresses [9]. For instance, *RBOHA* and *RBOHD* are required for the accumulation of ROS during the plant defense response against cold stress in strawberries [59]. Moreover, the expression levels of *VvRBOHA* and *VvRBOHB* were significantly increased in grapes upon salt and drought stress treatments [9]. Further existing studies confirmed that, H_2O_2 enhances thermotolerance; therefore mutations in the ROS-generating *RBOHs* may cause defects in plant thermotolerance [7]. Similarly, in our investigation, transient overexpression of *GhCDPK16* in cotton decreased MDA and H_2O_2 were found to be increased significantly under heat stress, whereas Cas9:*GhCDPK16* plants sowed enhanced concentrations of ROS compounds. In addition, tested antioxidant activities were higher in overexpressed lines than in Cas9:*GhCDPK16* plants, signifying that *GhCDPK16* may have played a role in ROS scavenging and protection of leave membrane damages (Figs. 7 and 9). Thus, we hypothesized that H_2O_2 and its regulatory gene may have role in cotton tolerance to heat stress. In addition to *RBOH* proteins, Other heat stress-related proteins interacted with the *GhCDPK* gene, including *LRR*, *HsfA3*, and *CML*-related calcium ion-binding protein, known to control heat sensors [60] and regulate the heat stress response in *Arabidopsis* [61].

Thermotolerance is significantly influenced by the abscisic acid (ABA) hormone. Also, the *WRKY* TFs play a triggering role in activating ABA hormone signals [62]. In *Arabidopsis*, calcineurin B-like protein 9 (*CBL9*) was reported to be a calcium sensor involved in abscisic acid (ABA) signaling and stress-induced ABA biosynthesis pathways [63]. Similarly, a loss of *WRKY33* function resulted in elevated ABA levels [62]. Moreover, *Arabidopsis AtWRKY25*, *AtWRKY26*, and *AtWRKY33* promote the expression of ethylene insensitive protein 2 (EIN2) and the ethylene-mediated signal transduction pathway, thereby improving the high-temperature tolerance of plants [55]. Here, *CBL9* and *WRKY33* proteins interacted with *GhCDPK16*. We speculate that *GhCDPK16* may have interacted with *WRKY* and *CBL* proteins to induce hormonal tolerance by regulating ABA and ethylene levels, during heat stress. Crizel et al. [9] further reported that *FaCDPK4* and *FaCDPK11* utilize ABA as the signaling molecule to increase the content of phenolics, ascorbic acid, and sugar compounds involved in drought stress tolerance. The ABA-mediated AsA-GSH promotes regeneration and improves the antioxidant capacity, alleviates the damage of ROS, reduces growth inhibition, and enhances the tolerance of desiccation stress [64]. Moreover, ABA acts as a defensive stress hormone against plant heat stress by inducing endogenous ABA content,

which promotes water balance and strengthens heat tolerance [65]. Under extreme temperatures of 42 °C, 48 h in *Vicia faba* L and 38/28°C day/night, 7 days in *L. esculentum* Mill, the AsA, GSH, GSSG, AsA+DHA, and DHA content significantly increased [66]. Consistent with the current study, antioxidant concentrations in the leaves of the transgenic line significantly increased compared to the wild-type, indicating the activation of antioxidant protection (Fig. 8). Furthermore, we speculated that ABA might have played a role in the control of endogenous antioxidant levels.

Conclusions

In this study, a total of 48 predicted CDPKs were identified from upland cotton (*Gossypium hirsutum* L.), and phylogenetic analyses classified them into three groups. All CDPK proteins are localized in the nucleus and contain EF-hand motifs and kinase structural domains. The predicted *ERF*, *MYB*, and *WRKY* transcription binding sites showed the possibility of abiotic stress tolerance. Significant expression profiles of *GhCDPK16/19* during 24 h of heat stress indicated a connection with heat stress responses. Moreover, the protein-protein interaction network analysis highlighted proteins involved in ROS regulation, heat stress TFs, and ABA-dependent Ca^{2+} signaling. Transient overexpression of *GhCDPK16* in cotton and permanent overexpression in *Arabidopsis* substantially reduced H_2O_2 content and augmented tolerance by increasing protective antioxidant enzymes through ROS scavenging. This study provides a basis for subsequent studies on the functions of the *GhCDPK16* gene family members in cotton and provides a theoretical basis for breeding new heat-tolerant cotton varieties. We propose future functional genomic studies on the interactive role of *GhCDPK16* with heat stress-responsive proteins, which will allow deeper elucidation of the *GhCDPK16* role in plant heat stress tolerance.

Appendix A. Supporting information

Additional supporting information may be found online in the Supporting Information section at the end of the article.

Abbreviations

CDPK	Calcium-dependent protein kinase
BLAST	Basic Local Alignment Search tool
Aa	Amino acids
KDa	Kilo Dalton
pI	Protein Isoelectric Point
ABA	Abscisic Acid
IAA	Auxin
KDa	Kilo
GA	Gibberellin
MeJA	Methyl Jasmonate
SA	Salicylic Acid
ERF	Ethylene Responsive Transcription Factor
ABRE	Abscisic Acid Responsiveness Element
LRT	Low Temperature Response
MBS	MYB Binding Site
RY-element	Seed specifc regulation
O2-site	Zein metabolism regulation elements
Ox	Overexpression
qRT-PCR	Quantitative Real-time Polymerase Chain Reaction
CAT	Catalase
POD	Peroxidase
SOD	Superoxide Dismutase
ROD	Reactive Oxygen Species
WT	Wild Type
TFs	Transcription Factors
TFBDS	Transcription Factor Binding Site

Supplementary Information

The online version contains supplementary material available at https://doi.org/10.1186/s12870-024-05563-x.

Supplementary Material 1

Supplementary Material 2

Supplementary Material 3

Supplementary Material 4

Acknowledgements

Not applicable.

Author contributions

WBL and JSG conceived and designed the experiments. WBL and MCS finished the main experiments. CHD, YTC, ML and AGO analyzed the data. WBL and CCM wrote the manuscript. JSG and AGO revised the manuscript. NG and DHL guided the experiments.

Funding

This work was supported by State Key Laboratory of Cotton Bio-breeding and Integrated Utilization and Sponsored by State Key Laboratory of Cotton Bio-breeding and Integrated Utilization Open Fund (*CB2024A12)*.

Data availability

The data provided within the manuscript or supplementary information of this article will be made available by the corresponding authors, without undue reservation.

Declarations

Competing interests

The authors declare no competing interests.

Consent of publication

Not applicable.

Received: 17 February 2024 / Accepted: 2 September 2024
Published online: 07 September 2024

References

1. Arshad MS, Farooq M, Asch F, Krishna JSV, Prasad PVV, Siddique KHM, et al. Thermal stress impacts Reproductive Development and Grain Yield in Rice. Plant Physiol Biochem. 2017;115(3):57–72.
2. Huang LZ, Zhou M, Ding YF, Zhu C, et al. Gene Networks Involved in Plant Heat Stress Response and tolerance. Int J Mol Sci. 2022;23(19):1–19.
3. Kim JH, Lim SD, Jang CS, et al. Oryza Sativa Heat-Induced RING finger protein 1 (OsHIRP1) positively regulates Plant Response to heat stress. Plant Mol Biol. 2019;99(6):545–59.
4. Guo LM, Li J, He J, Liu H, Zhang HM, et al. A class I cytosolic HSP20 of Rice enhances Heat and Salt Tolerance in different organisms. Sci Rep. 2020;10(1):1–13.

5. Feng ZJ, Liu N, Zhang GW, Niu FG, Xu SC, Gong YM, et al. Investigation of the AQP family in soybean and the promoter activity of TIP2;6 in heat stress and hormone responses. Int J Mol Sci. 2019;20(2):1–19.
6. Song Y, Chen P, Liu P, Bu C, Zhang D, et al. High-temperature-responsive Poplar LncRNAs modulate target gene expression via RNA interference and act as RNA scaffolds to Enhance Heat Tolerance. Int J Mol Sci. 2020;21(18):1–22.
7. Zhao Y, Du H, Wang Y, Wang H, Yang S, Li C, Chen N, Yang H, Zhang Y, Zhu Y, Yang L, Hu X, et al. The calcium-dependent protein kinase ZmCDPK7 functions in heat-stress tolerance in Maize. J Integr Plant Biol. 2021;63(3):510–27.
8. Wang H, Niu H, Liang M, Zhai Y, Huang W, Ding Q, Du Y, Lu M, et al. A Wall-Associated kinase gene Cawakl20 from Pepper negatively modulates Plant Thermotolerance by reducing the expression of ABA-Responsive genes. Front Plant Sci. 2019;10(5):1–13.
9. Crizel RL, Perin EC, Vighi IL, Woloski R, Seixas A, da Silva Pinto L, Rombaldi CV, Galli V, et al. Genome-wide identification, and characterization of the CDPK Gene Family Reveal their involvement in Abiotic Stress Response in Fragaria x Ananassa. Sci Rep. 2020;10(1):1–17.
10. Edel KH, Marchadier E, Brownlee C, Kudla J, Hetherington AM, et al. The evolution of calcium-based signalling in plants. Curr Biol. 2017;27(13):R667–79.
11. Valmonte GR, Arthur K, Higgins CM, Macdiarmid RM, et al. Calcium-dependent protein kinases in plants: evolution, expression and function. Plant Cell Physiol. 2014;55(3):551–69.
12. Klimecka M, Muszyńska G, et al. Structure and functions of Plant Calcium-Dependent protein kinases. Acta Biochim Pol. 2007;54(2):219–33.
13. Giammaria V, Grandellis C, Bachmann S, Gargantini PR, Feingold SE, Bryan G, Ulloa RM, et al. StCDPK2 expression and activity reveal a highly responsive potato calcium-dependent protein kinase involved in light signalling. Planta. 2011;233(3):593–609.
14. Xu J, Tian YS, Peng RH, Xiong AS, Zhu B, Jin XF, Gao F, Fu XY, Hou XL, Yao QH, et al. AtCPK6, a functionally redundant and positive Regulator involved in Salt/Drought stress tolerance in Arabidopsis. Planta. 2010;231(6):1251–60.
15. Liu HT, Gao F, Li GL, Han JL, Liu DL, Sun DY, Zhou RG, et al. The calmodulin-binding protein kinase 3 is part of Heat-Shock Signal Transduction in Arabidopsis Thaliana. Plant J. 2008;55(5):760–73.
16. Dubrovina AS, Kiselev KV, Khristenko VS, Aleynova OA, et al. The calcium-dependent protein kinase gene VaCPK29 is involved in grapevine responses to heat and osmotic stresses. Plant Growth Regul. 2017;82(1):79–89.
17. Yan M, Yu X, Zhou G, Sun D, Hu Y, Huang C, Zheng Q, Sun N, Wu J, Fu Z, Li L, Feng Z, Yu S, et al. GhCDPK60 positively regulates Drought stress tolerance in both transgenic Arabidopsis and Cotton by regulating Proline Content and ROS Level. Front. Plant Sci. 2022;13(12):1–15.
18. Yan R, Liang C, Meng Z, Malik W, Zhu T, Zong X, Guo S, Zhang R, et al. Progress in genome sequencing will accelerate molecular breeding in cotton (Gossypium Spp). 3 Biotech. 2016;6(2):1–9.
19. Zahid KR, Ali F, Shah F, Younas M, Shah T, Shahwar D, Hassan W, Ahmad Z, Qi C, Lu Y, Iqbal A, Wu W, et al. Response and tolerance mechanism of Cotton Gossypium Hirsutum L. to elevated temperature stress: a review. Front. Plant Sci. 2016;7(6):1–13.
20. Owusu AG, Lv Y-P, Liu M, Wu Y, Li C-L, Guo N, Li D-H, Gao J-S, et al. Transcriptomic and metabolomic analyses reveal the potential mechanism of Waterlogging Resistance in Cotton (Gossypium Hirsutum L.). Front. Plant Sci. 2023;14(6):1–17.
21. Liu W, Li W, He Q, Daud MK, Chen J, Zhu S, et al. Genome-wide survey and expression analysis of calcium-dependent protein kinase in Gossypium Raimondii. PLoS ONE. 2014;9(6):1–11.
22. Zhang T, Hu Y, Jiang W, Fang L, Guan X, Chen J, Zhang J, Saski CA, Scheffler BE, Stelly DM, Hulse-Kemp AM, Wan Q, Liu B, Liu C, Wang S, Pan M, Wang Y, Wang D, Ye W, Chang L, Zhang W, Song Q, Kirkbride RC, Chen X, Dennis E, Llewellyn DJ, Peterson DG, Thaxton P, Jones DC, Wang Q, Xu X, Zhang H, Wu H, Zhou L, Mei G, Chen S, Tian Y, Xiang D, Li X, Ding J, Zuo Q, Tao L, Liu Y, Li J, Lin Y, Hui Y, Cao Z, Cai C, Zhu X, Jiang Z, Zhou B, Guo W, Li R, Chen ZJ, et al. Sequencing of Allotetraploid Cotton (Gossypium Hirsutum L. Acc. TM-1) provides a resource for Fiber improvement. Nat Biotechnol. 2015;33(5):531–7.
23. Tamura K, Stecher G, Peterson D, Filipski A, Kumar S, et al. MEGA6: Molecular Evolutionary Genetics Analysis Version 6.0. Mol Biol Evol. 2013;30(12):2725–9.
24. Shi G, Zhu X, et al. Genome-wide identification and functional characterization of CDPK Gene Family Reveal their involvement in response to Drought stress in Gossypium Barbadense. PeerJ. 2022;10(2):1–20.
25. Gao C, Gao K, Yang H, Ju T, Zhu J, Tang Z, Zhao L, Chen Q, et al. Genome-wide analysis of Metallothionein Gene Family in Maize to Reveal its role in development and stress resistance to Heavy Metal. Biol Res. 2022;55(1):1–13.
26. Jiang Z, Zhang H, Gao S, Zhai H, He S, Zhao N, Liu Q, et al. Genome-wide identification and expression analysis of the sucrose synthase Gene Family in Sweet Potato and its two diploid relatives. Int J Mol Sci. 2023;24(15):1–18.
27. Hui W, Zheng H, Fan J, Wang J, Saba T, Wang K, Wu J, Wu H, Zhong Y, Chen G, Gong W, et al. Genome-wide characterization of the MBF1 Gene Family and its expression pattern in different tissues and stresses in Zanthoxylum Armatum. BMC Genomics. 2022;23(1):1–21.
28. Yang Z, Zhang R, Zhou Z, et al. The XTH Gene Family in Schima Superba: genome-wide identification, expression profiles, and Functional Interaction Network Analysis. Front. Plant Sci. 2022;13(6):1–15.
29. Alok A, Chauhan H, Upadhyay SK, Pandey A, Kumar J, Singh K, et al. Compendium of Plant-Specific CRISPR vectors and their technical advantages. Life. 2021;11(10):1–19.
30. Sun S, Xiong X, Zhang X, Feng H, Zhu Q, Sun J, et al. Characterization of the Gh4CL Gene Family reveals a role of Gh4CL7 in Drought Tolerance. BMC Plant Biol. 2021;20(2020):1–15.
31. Wen Z, Chen Z, Liu X, Sun J, Zhang F, Zhang M, Dong C, et al. 24-Epibrassinolide facilitates adventitious Root formation by coordinating cell-wall polyamine oxidase- and plasma membrane respiratory burst oxidase homologue-derived reactive oxygen species in Capsicum Annuum L. Antioxidants. 2023;12(7):1–22.
32. Li P, Cai Q, Wang H, Li S, Cheng J, Li H, Yu Q, Wu S, et al. Hydrogen Peroxide Homeostasis provides beneficial Micro-environment for SHR-Mediated Periclinal Division in Arabidopsis Root. New Phytol. 2020;228(6):1926–38.
33. Sarker U, Oba S, et al. Catalase, Superoxide dismutase and ascorbate-glutathione cycle enzymes Confer Drought Tolerance of Amaranthus Tricolor. Sci Rep. 2018;8(1):1–12.
34. Zhou H, Zhou KH, Zhao G, Wang PP, Yang DG, Ma XF, Gao JS, et al. Physiological and biochemical properties of Cotton seedlings in response to Cu2 + stress. Curr Issues Mol Biol. 2023;45(5):4050–62.
35. Noctor G, Mhamdi A, Foyer CH, et al. Oxidative stress and Antioxidative systems: recipes for successful data Collection and Interpretation. Plant Cell Environ. 2016;39(5):1140–60.
36. Niu M-X, Feng C-H, Liu M, Liu X, Liu S, Liu C, Yin W, Xia X, et al. Genome-wide identification of Poplar GSTU Gene Family and its PtrGSTU23 and PtrGSTU40 to Improve Salt Tolerance in Poplar. Ind Crops Prod. 2024;209(10):1–14.
37. Hetherington A, Trewavas A, et al. Calcium-dependent protein kinase in pea shoot membranes. FEBS Lett. 1982;145(1):67–71.
38. Li Lbei, Yu D, wei, Zhao F, li, Pang C you, Song M, zhen, Wei H ling, Fan S li, Yu S et al. xun,. Genome-Wide Analysis of the Calcium-Dependent Protein Kinase Gene Family in Gossypium Raimondii. J. Integr. Agric. 2015; 14(1): 29–41.
39. Wu Y, Zhang L, Zhou J, Zhang X, Feng Z, Wei F, Zhao L, Zhang Y, Feng H, Zhu H, et al. Calcium-dependent protein kinase GhCDPK28 was dentified and involved in Verticillium Wilt Resistance in Cotton. Front Plant Sci. 2021;12(11):1–19.
40. Gao W, Xu FC, Guo DD, Zhao JR, Liu J, Guo YW, Singh PK, Ma XN, Long L, Botella JR, Song CP, et al. Calcium-dependent protein kinases in cotton: insights into early plant responses to salt stress. BMC Plant Biol. 2018;18(1):1–15.
41. Ma SY, Wu WH, et al. AtCPK23 functions in Arabidopsis responses to Drought and Salt stresses. Plant Mol Biol. 2007;65(4):511–8.
42. Wen F, Ye F, Xiao Z, Liao L, Li T, Jia M, Liu X, Wu X, et al. Genome-wide survey and expression analysis of calcium-dependent protein kinase (CDPK) in Grass Brachypodium Distachyon. BMC Genomics. 2020;21(1):1–17.
43. Thornton JW, Desalle R, et al. GENE FAMILY EVOLUTION AND HOMOLOGY: Genomics meets phylogenetics. New York. 2000;1(48):41–73.
44. Wang CT, Shao JM, et al. Characterization of the ZmCK1 gene encoding a calcium-dependent protein kinase responsive to multiple abiotic stresses in Maize. Plant Mol Biol Rep. 2013;31(1):222–30.
45. Asai S, Ichikawa T, Nomura H, Kobayashi M, Kamiyoshihara Y, Mori H, Kadota Y, Zipfel C, Jones JDG, Yoshioka H, et al. The variable domain of a plant calcium-dependent protein kinase (CDPK) confers subcellular localization and substrate recognition for NADPH oxidase. J Biol Chem. 2013;288(20):14332–40.
46. Yang H, Zhou Y, Zhang Y, Wang J, Shi H, et al. Identification of Transcription Factors of Nitrate Reductase Gene Promoters and NRE2 Cis-element through yeast one-hybrid screening in Nicotiana Tabacum. BMC Plant Biol. 2019;19(1):1–8.
47. Li J, Chen X, Zhou X, Huang H, Wu D, Shao J, Zhan R, Chen L, et al. Identification of Trihelix Transcription Factors in Pogostemon Cablin reveals PatGT-1 negatively regulates Patchoulol Biosynthesis. Ind Crops Prod. 2021;161(7):113182.

48. Cao Z, He Q, Wang P, Yan J, Awais MM, Liu Z, Yan H, Sun J, et al. Functional characteristics of a calcium-dependent protein kinase (MaCDPK1) Enduring stress tolerance from Morus Atropurpurea Roxb. Plant Cell Tissue Organ Cult. 2020;141(1):131–43.
49. Li W, Cui X, Meng Z, Huang X, Xie Q, Wu H, Jin H, Zhang D, Liang W et al. Transcriptional regulation of Arabidopsis MIR168a and ARGONAUTE1 Homeostasis in Abscisic Acid and Abiotic stress responses, vol. 158. 2012.
50. Zhu C, Schraut D, Hartung W, Schäffner AR, et al. Differential responses of Maize MIP genes to salt stress and ABA. J Exp Bot. 2005;56(421):2971–81.
51. Lai X, Stigliani A, Vachon G, Carles C, Smaczniak C, Zubieta C, Kaufmann K, Parcy F, et al. Building transcription factor binding site models to understand gene regulation in plants. Mol Plant. 2019;12(6):743–63.
52. Licausi F, Ohme-Takagi M, Perata P, et al. APETALA2/Ethylene Responsive factor (AP2/ERF) transcription factors: mediators of stress responses and Developmental Programs. New Phytol. 2013;199(3):639–49.
53. Huang J, Zhao X, Bürger M, Wang Y, Chory J, et al. Two interacting Ethylene response factors regulate heat stress response. Plant Cell. 2021;33(2):338–57.
54. El-kereamy A, Bi YM, Ranathunge K, Beatty PH, Good AG, Rothstein SJ, et al. The Rice R2R3-MYB transcription factor OsMYB55 is involved in the tolerance to high temperature and modulates amino acid metabolism. PLoS ONE. 2012;7(12):1–16.
55. Cheng Z, Luan Y, Meng J, Sun J, Tao J, Zhao D, et al. WRKY Transcription Factor Response to high-temperature stress. Plants. 2021;10(10):1–13.
56. Tong Y, Huang H, Wang Y, et al. Genome-wide analysis of the Trihelix Gene Family and their response to cold stress in Dendrobium Officinale. Sustain. 2021;13(5):1–15.
57. Alshareef NO, Otterbach SL, Allu AD, Woo YH, de Werk T, Kamranfar I, Mueller-Roeber B, Tester M, Balazadeh S, Schmöckel SM, et al. NAC Transcription Factors ATAF1 and ANAC055 affect the heat stress response in Arabidopsis. Sci Rep. 2022;12(1):1–15.
58. Yang M, He G, Hou Q, Fan Y, Duan L, Li K, Wei X, Qiu Z, Chen E, He T, et al. Systematic analysis and expression profiles of TCP Gene Family in Tartary Buckwheat (Fagopyrum Tataricum (L.) Gaertn.) Revealed the potential function of FtTCP15 and FtTCP18 in response to Abiotic Stress. BMC Genomics. 2022;23(1):1–19.
59. Zhang Y, Li Y, He Y, Hu W, Zhang Y, Wang X, Tang H, et al. Identification of NADPH oxidase Family Members Associated with Cold stress in Strawberry. FEBS Open Bio. 2018;8(4):593–605.
60. Marchetti F, Cainzos M, Cascallares M, Distéfano AM, Setzes N, López GA, Zabaleta E, Pagnussat GC, et al. Heat stress in Marchantia Polymorpha: sensing and mechanisms underlying a dynamic response. Plant Cell Environ. 2021;44(7):2134–49.
61. Schramm F, Larkindale J, Kiehlmann E, Ganguli A, Englich G, Vierling E, Von Koskull-Döring P, et al. A Cascade of transcription factor DREB2A and heat stress transcription factor HsfA3 regulates the heat stress response of Arabidopsis. Plant J. 2008;53(2):264–74.
62. Liu S, Kracher B, Ziegler J, Birkenbihl RP, Somssich IE, et al. Negative regulation of ABA signaling by WRKY33 is critical for Arabidopsis Immunity towards Botrytis Cinerea 2100. Elife. 2015;4(6):1–27.
63. Pandey GK, Yong HC, Kim KN, Grant JJ, Li L, Hung W, D'Angelo C, Weinl S, Kudla J, Luan S, et al. The Calcium Sensor Calcineurin B-like 9 modulates abscisic acid sensitivity and biosynthesis in Arabidopsis. Plant Cell. 2004;16(7):1912–24.
64. Jiang Z, Zhu H, Zhu H, Tao Y, Liu C, Liu J, Yang F, Li M, et al. Exogenous ABA enhances the antioxidant Defense System of Maize by regulating the AsA-GSH cycle under Drought stress. Sustain. 2022;14(5):1–15.
65. Sezgin Muslu A, Kadıoğlu A, et al. Role of Abscisic Acid, Osmolytes and Heat Shock factors in high temperature thermotolerance of Heliotropium Thermophilum. Physiol Mol Biol Plants. 2021;27(4):861–71.
66. Hasanuzzaman M, Borhannuddin Bhuyan MHM, Anee TI, Parvin K, Nahar K, Al Mahmud J, Fujita M, et al. Regulation of ascorbate-glutathione pathway in mitigating oxidative damage in plants under abiotic stress. Antioxidants. 2019;8(9):1–50.

Publisher's note